

**OFFICE OF CIVILIAN RADIOACTIVE WASTE MANAGEMENT
CALCULATION COVER SHEET**

1. QA: QA

Page: 1 Of: 32

2. Calculation Title
Horizontal Drop of 21-PWR Waste Package

3. Document Identifier (including Revision Number)
CAL-UDC-ME-000009 REV 01

4. Total Attachments

2

5. Attachment Numbers - Number of pages in each
I-25, II on Compact Disc (CD)

	Print Name	Signature	Date
6. Originator	Adam K. Scheider	<i>Adam K. Scheider</i>	APR 26, 2001
7. Checker	Timothy Schmitt	<i>Tim Schmitt</i>	Apr. 27, 2001
8. Lead	Scott M. Bennett	<i>Scott M. Bennett</i>	05/02/01

9. Remarks

None

Revision History

10. Revision No.	11. Description of Revision
00	Initial Issuance.
01	Inner Shell top lid changed to Shear Ring design. The temperature cases analyzed used ASME elongation values at 70, 400, and 600 degrees Fahrenheit. A fourth case was analyzed at 600 degrees Fahrenheit using vendor elongation data to provide a range of possible results.

CONTENTS

	Page
1. PURPOSE	4
2. METHOD.....	4
3. ASSUMPTIONS.....	4
4. USE OF COMPUTER SOFTWARE AND MODELS.....	6
4.1 SOFTWARE	6
4.2 SOFTWARE ROUTINES	6
4.3 MODELS	6
5. CALCULATION	7
5.1 MASS AND GEOMETRIC DIMENSIONS OF WASTE PACKAGE	7
5.2 MATERIAL PROPERTIES	7
5.2.1 Calculations for Elevated-Temperature Material Properties.....	9
5.2.2 Calculations for True Measures of Ductility.....	9
5.2.3 Calculations for Tangent Moduli.....	12
5.3 INITIAL VELOCITY OF WASTE PACKAGE	14
5.4 FINITE ELEMENT REPRESENTATION	15
6. RESULTS.....	16
7. REFERENCES.....	30
8. ATTACHMENTS	32

FIGURES

	Page
1. Horizontal Drop Geometry.....	14
2. Inner Shell Stresses at Room Temperature	17
3. Inner Shell Stresses at 400 °F.....	18
4. Inner Shell Stresses at 600 °F.....	19
5. Inner Shell Stresses at 600 °F Using Vendor Elongation Values	20
6. Outer Shell Maximum Stresses at Room Temperature.....	21
7. Outer Shell Maximum Stresses at 400 °F	22
8. Outer Shell Maximum Stresses at 600 °F	23
9. Outer Shell Maximum Stresses at 600 °F Using Vendor Elongation	24
10. Shear Ring Maximum Stresses at Room Temperature	25
11. Shear Ring Maximum Stresses at 400 °F.....	26
12. Shear Ring Maximum Stresses at 600 °F.....	27
13. Shear Ring Maximum Stresses at 600 °F Using Vendor Elongation.....	28

TABLES

6-1. Maximum Stress Intensity by Load Case	29
8-1. List of Attachments Submitted in the Form of Electronic Files in Attachment II.....	32

1. PURPOSE

The objective of this calculation is to determine the structural response of the waste package (WP) dropped horizontally from a specified height. The WP used for that purpose is the 21-Pressurized Water Reactor (PWR) WP. The scope of this document is limited to reporting the calculation results in terms of stress intensities. The information provided by the sketches (Attachment I) is that of the potential design of the type of WP considered in this calculation, and all obtained results are valid for that design only. This calculation is associated with the WP design and was performed by the Waste Package Design group in accordance with the *Technical Work Plan for: Waste Package Design Description for LA* (Ref. 16). AP-3.12Q, *Calculations* (Ref. 11) is used to perform the calculation and develop the document. The sketches attached to this calculation provide the potential dimensions and materials for the 21-PWR WP design.

2. METHOD

The finite element calculation was performed by using the commercially available ANSYS Version (V) 5.6.2 (Software Tracking Number [STN] 10364-5.6.2-00; Ref. 4) and LS-DYNA V950.C (STN 10300-950-00; Ref. 7) finite element codes. The results of this calculation were provided in terms of maximum stress intensities in the outer shell (OS), inner shell (IS), and Shear Ring.

With regard to the development of this calculation, the control of electronic management of data was evaluated in accordance with AP-SV.1Q, *Control of the Electronic Management of Information* (Ref. 10) and the Technical Work Plan (Ref. 16). The evaluation (Addendum B of Ref. 16) determined that current work processes and procedures are adequate for the control of the electronic management of data for this activity.

3. ASSUMPTIONS

In the course of developing this document, the following assumptions are made regarding the structural calculation.

- 3.1 Some of the temperature-dependent material properties, such as Poisson's Ratio, Coefficient of Thermal Expansion, and density, are not available for SB-575 N06022 (Alloy 22), SA-516 K02700 (516 carbon steel [CS]), and SA-240 S31600 (316 stainless steel [SS]). The room-temperature (20 °C) material properties are assumed for both materials. The impact of using room-temperature material properties is anticipated to be small. The rationale for this assumption is that undetermined material properties of said materials will not significantly impact the results. This assumption is used in Section 5.2.
- 3.2 The Poisson's ratio of Alloy 22 is not available in literature. The Poisson's ratio of Alloy 625 (SB-443 N06625) is assumed for Alloy 22. The impact of this assumption is anticipated to be negligible. The rationale for this assumption is that the chemical compositions of Alloy 22 and Alloy 625 are similar (see Ref. 2, SB-575 Table 1 and Ref. 13, p. 143, respectively). This assumption is used in Section 5.2.

3.3 Some of the rate-dependent material properties are not available for SB-575 N06022 (Alloy 22), SA-516 K02700 (516 carbon steel [CS]), and SA-240 S31600 (316 stainless steel [SS]). Linear approximations are assumed for all materials. The impact of using such an approximation is anticipated to be small. The rationale for this assumption is that this is the most common and accepted way of approximating these properties. This assumption is used in Section 5.2.

3.4 Poisson's ratio is not available for 516 CS. Therefore, Poisson's ratio of cast carbon steel is assumed for 516 CS. The impact of this assumption is anticipated to be negligible. The rationale for this assumption is that the elastic constants of cast carbon steels are only slightly affected by changes in composition and structure (see Ref. 3). This assumption is used in Section 5.2.

3.5 The exact geometry of the loaded internals is simplified for the purpose of this calculation. The spent fuel was modeled as 21 separate solid rectangles made from SS304L, but the thermal shunts, fuel tubes, and dividers between the fuel assemblies were omitted. The density of the spent fuel was increased to account for the missing mass. However, the sideguides, cornerguides, and stiffeners were included to accurately represent the contact with the inner shell. The rationale for this assumption is to simplify the finite element representation (FER), thus reducing processing time and file size, without compromising the accuracy of the calculation. This assumption is used in Section 5.4 and Section 5.2.

3.6 The elongations of Alloy 22 and 316NG SS at elevated temperatures are not available from traditional sources. However, vendor data is available (Ref. 6 and Ref. 17). The percent difference between elongations at room temperature and elevated temperatures can be normalized and applied to the data available from accepted codes. The rationale for this assumption is that the relative change of typical elongations should be bounding for the relative change of minimum elongation. Even though the values are not from traditional sources, the values are conservative and create higher stress intensities for the same temperature. This assumption is used in Section 5.2.1.

3.7 The impact surface that the WP is to be dropped on is conservatively assumed to be perfectly rigid (unyielding). Such a material does not exist. LS-DYNA is able to simulate such a surface. The result will be that the stresses produced by this calculation will be small percentage higher than those that would result if a realistic surface were used. The rationale is that this is a conservative assumption. This assumption is used in Section 5.4.

3.8 Three-stage deformation characteristics are not observed in the stress-strain curves for Alloy 22 or Type 316 stainless steel (Ref. 12). However, in order to capture the uniform strain of the material from the curves, the total elongation should be conservatively reduced by 10%. The rationale for this assumption is to truncate the last portion of the curve that has decreasing slope. This assumption is used in Section 5.2.2.

3.9 The uniform strain of A 516 Grade 70 CS is not available in literature. Therefore, it is conservatively assumed that the uniform strain is 50% of its elongation. The rationale for this assumption is the stress-strain curve for A 36 CS (see Refs. 5 and 8), which has similar chemical composition with A 516 Grade 70 CS (see Ref. 2, SA-516/SA-516M and SA-36/SA-36M), displays uniform strain which is 50% of its elongation. This assumption is used in Section 5.2.2.

4. USE OF COMPUTER SOFTWARE AND MODELS

4.1 SOFTWARE

The first finite element analysis (FEA) computer code used for this calculation is ANSYS V5.6.2 (Ref. 4), which is identified with the Software Tracking number (STN) 10364-5.6.2-00 and was obtained from Software Configuration Management in accordance with appropriate procedures. ANSYS V5.6.2 is a commercially available finite element analysis code and is appropriate for structural calculations of WPs as performed in this calculation. The calculations using the ANSYS V5.6.2 software were executed on a Hewlett-Packard (HP) 9000 Series UNIX workstation, Yucca Mountain Project (YMP) tag number 700314 located in Las Vegas, NV. The ANSYS evaluations performed for these designs are fully within the range of the validation performed for the ANSYS V5.6.2 code. Access to the code was granted by the Software Configuration Secretariat in accordance with the appropriate procedures.

The second FEA code used is Livermore Software Technology Corporation (LSTC) LS-DYNA V950.C (Ref. 7). LS-DYNA V950.C was obtained from the Software Configuration Secretariat in accordance with the appropriate procedures and is identified by STN 10300-950-00. LS-DYNA V950.C is appropriate for its intended use. The LS-DYNA evaluation performed for this calculation is fully within the range of the validation performed for the LS-DYNA V950.C code. The calculations were executed on HP 9000 series UNIX workstations identified with YMP tag numbers 117161 and 117162 located in Las Vegas, NV.

The input and output files are defined in Section 8 of this document. They are located in Attachment II to this document.

4.2 SOFTWARE ROUTINES

None used.

4.3 MODELS

None used.

5. CALCULATION

5.1 MASS AND GEOMETRIC DIMENSIONS OF WASTE PACKAGE

This calculation was performed using mass and geometric dimensions of the 21-PWR waste package (see pp. I-1, I-15, and I-24):

Total mass of the loaded WP = 41,598 kg

Length = 5.129 m

Outer diameter of outer shell = 1.574 m

Outer diameter of trunnion collar sleeve = 1.654 m

5.2 MATERIAL PROPERTIES

Material properties used in these calculations are listed in this section. Some of the temperature-dependent and rate-dependent material properties are not available for Alloy 22, 316NG SS, and 516 CS. Therefore, room-temperature density and Poisson's ratio obtained under the static loading conditions are used for Alloy 22, 316NG SS, and 516 CS (see Assumptions 3.1 and 3.3). All references to Ref. 2 in this Section are from Section II of Ref. 2.

SB-575 N06022 (Alloy 22) (Outer shell, outer shell lids, upper and lower trunnion collar sleeves):

- ⌚ Density = 8690 kg/m³ (0.314 lb/in³) (at room temperature) (Ref. 2, SB-575 Section 7.1)
- ⌚ Yield strength = 310 MPa (45 ksi) (at room temperature) (Ref. 2, Table Y-1)
Yield strength = 236 MPa (34.3 ksi) (at 400 °F = 204 °C) (Ref. 2, Table Y-1)
Yield strength = 211 MPa (30.6 ksi) (at 600 °F = 316 °C) (Ref. 2, Table Y-1)
- ⌚ Tensile strength = 690 MPa (100 ksi) (at room temperature) (Ref. 2, Table U)
Tensile strength = 657 MPa (95.3 ksi) (at 400 °F = 204 °C) (Ref. 2, Table U)
Tensile strength = 628 MPa (91.1 ksi) (at 600 °F = 316 °C) (Ref. 2, Table U)
- ⌚ Elongation = 0.45 (at room temperature) (Ref. 2, SB-575 Table 3)
- ⌚ Poisson's ratio = 0.278 (at room temperature) (Ref. 13, p. 143; see Assumption 3.2)
- ⌚ Modulus of elasticity = 206 GPa (at room temperature) (Ref. 6, p. 14)
Modulus of elasticity = 196 GPa (at 400 °F = 204 °C) (Ref. 6, p. 14)
Modulus of elasticity = 190 GPa (at 600 °F = 316 °C) (Ref. 6, p. 14)

SA-240 S31600 (316NG SS, which is 316 SS with tightened control on carbon and nitrogen content and has the same material properties as 316 SS [see Ref. 18, page 931 and Ref. 2, Section II, SA-240 Table 1]) (Inner shell, inner shell lids, and inner shell lifting feature):

- ⌚ Density = 7980 kg/m³ (at room temperature) (Ref. 14, Table X1, p. 7)

- Yield strength = 207 MPa (30 ksi) (at room temperature) (Ref. 2, Table Y-1)
Yield strength = 148 MPa (21.4 ksi) (at 400 °F = 204 °C) (Ref. 2, Table Y-1)
Yield strength = 130 MPa (18.9 ksi) (at 600 °F = 316 °C) (Ref. 2, Table Y-1)
- Tensile strength = 517 MPa (75 ksi) (at room temperature) (Ref. 2, Table U)
Tensile strength = 496 MPa (71.9 ksi) (at 400 °F = 204 °C) (Ref. 2, Table U)
Tensile strength = 495 MPa (71.8 ksi) (at 600 °F = 316 °C) (Ref. 2, Table U)
- Elongation = 0.40 (at room temperature) (Ref. 2, SA-240 Table 2)
- Poisson's ratio = 0.298 (at room temperature) (Ref. 13, Figure 15, p. 755)
- Modulus of elasticity = 195 GPa (28.3 * 10⁶ psi) (at room temperature) (Ref. 2, Table TM-1)
Modulus of elasticity = 183 GPa (26.5 * 10⁶ psi) (at 400 °F = 204 °C) (Ref. 2, Table TM-1)
Modulus of elasticity = 174 GPa (25.3 * 10⁶ psi) (at 600 °F = 316 °C) (Ref. 2, Table TM-1)

SA-516 K02700 (516 CS) (Sideguides, stiffeners, and baskets):

- Density = 7850 kg/m³ (at room temperature) (Ref. 2, SA-20/SA20M, Section 14.1)
- Yield strength = 262 MPa (38 ksi) (at room temperature) (Ref. 2, Table Y-1)
Yield strength = 224 MPa (32.5 ksi) (at 400 °F = 204 °C) (Ref. 2, Table Y-1)
Yield strength = 201 MPa (29.1 ksi) (at 600 °F = 316 °C) (Ref. 2, Table Y-1)
- Tensile strength = 483 MPa (70 ksi) (at room temperature) (Ref. 2, Table U)
Tensile strength = 483 MPa (70 ksi) (at 400 °F = 204 °C) (Ref. 2, Table U)
Tensile strength = 483 MPa (70 ksi) (at 600 °F = 316 °C) (Ref. 2, Table U)
- Elongation = 0.21 (at room temperature) (Ref. 2, SA-516 Table 2)
- Poisson's ratio = 0.3 (at room temperature) (Ref. 3, p. 374) (see Assumption 3.4)
- Modulus of elasticity = 203 GPa (29.5 * 10⁶ psi) (at room temperature) (Ref. 2, Table TM-1)
Modulus of elasticity = 191 GPa (27.7 * 10⁶ psi) (at 400 °F = 204 °C) (Ref. 2, Table TM-1)
Modulus of elasticity = 184 GPa (26.7 * 10⁶ psi) (at 600 °F = 316 °C) (Ref. 2, Table TM-1)

SA-240 S30400 (304 SS) (21-PWR Fuel):

- Yield strength = 207 MPa (30 ksi) (at room temperature) (Ref. 2, Table Y-1)
Yield strength = 143 MPa (20.7 ksi) (at 400 °F = 204 °C) (Ref. 2, Table Y-1)
Yield strength = 127 MPa (18.4 ksi) (at 600 °F = 316 °C) (Ref. 2, Table Y-1)
- Tensile strength = 517 MPa (70 ksi) (at room temperature) (Ref. 2, Table U)
Tensile strength = 441 MPa (70 ksi) (at 400 °F = 204 °C) (Ref. 2, Table U)
Tensile strength = 437 MPa (70 ksi) (at 600 °F = 316 °C) (Ref. 2, Table U)

- ☐ Elongation = 0.40 (at room temperature) (Ref. 2, SA-240 Table 2)
- ☐ Poisson's ratio = 0.290 (at room temperature) (Ref. 13, Figure 15, p. 755)
- ☐ Modulus of elasticity = 195 GPa ($28.3 * 10^6$ psi) (at room temperature) (Ref. 2, Table TM-1)
Modulus of elasticity = 183 GPa ($26.5 * 10^6$ psi) (at 400 °F = 204 °C) (Ref. 2, Table TM-1)
Modulus of elasticity = 174 GPa ($25.3 * 10^6$ psi) (at 600 °F = 316 °C) (Ref. 2, Table TM-1)

5.2.1 Calculations for Elevated-Temperature Material Properties

The values for elongation at elevated temperatures are not listed in conventional listings such as American Society for Testing and Materials (ASTM) Standards or American Society of Mechanical Engineers (ASME) Boiler and Pressure Vessel Code. However, the elongation values at elevated temperatures are available from vendor data. This vendor data will be used to estimate elevated temperature elongation normalized to the room temperature values from accepted codes (see Assumption 3.6).

For Alloy 22, the vendor data shows an approximate 10% increase in elongation values between room temperature and 600 °F (Ref. 6). Therefore the elongation values for Alloy 22 at 600 °F will be as follows:

$$\text{Elongation}_{600\text{ °F}} = 0.45 * (1 + 0.10) = 0.50$$

For SS 316, the vendor data shows an approximate 30% decrease in elongation values between 600 °F and room temperature (Ref. 17).

Therefore the elongation values for SS 316 at 600 °F will be as follows:

$$\text{Elongation}_{600\text{ °F}} = 0.40 * (1 - 0.30) = 0.28$$

Since the components made of SA-516 and SS304 will not be analyzed for stresses, their elongations are not needed at elevated temperatures.

5.2.2 Calculations for True Measures of Ductility

The material properties in Sections 5.2 and 5.2.1 refer to engineering stress and strain definitions:

$$s = \frac{P}{A_0} \quad \text{and} \quad e = \frac{L - L_0}{L_0} \quad (\text{Ref. 15})$$

Where P stands for the force applied during static tensile test, L is the deformed-specimen length, and L_0 and A_0 are original length and cross-sectional area of specimen, respectively. It is generally accepted that the engineering stress-strain curve does not give a true indication of the

deformation characteristics of a material during the plastic deformation since it is based entirely on the original dimensions of the specimen. Therefore, the LS-DYNA V950.C finite element code requires input in terms of true stress and strain definitions:

$$\sigma = \frac{P}{A} \quad \text{and} \quad \epsilon = \ln\left(\frac{L}{L_0}\right) \quad (\text{Ref. 15})$$

The relationships between the true stress and strain definitions and engineering stress and strain definitions can be readily derived based on constancy of volume ($A_o * L_o = A * L$) and strain homogeneity during plastic deformation:

$$\sigma = s * (1 + e) \quad \text{and} \quad \epsilon = \ln(1 + e) \quad (\text{Ref. 15})$$

These expressions are applicable only in the hardening region of stress-strain curve that is limited by the onset of necking.

The following parameters are used in the subsequent calculations:

$s_y \approx \sigma_y \equiv$ yield strength

$s_u \equiv$ engineering tensile strength

$\sigma_u \equiv$ true tensile strength

$e_y \approx \epsilon_y \equiv$ strain corresponding to yield strength

$e_u \equiv$ engineering strain corresponding to tensile strength (engineering uniform strain)

$\epsilon_u \equiv$ true strain corresponding to tensile strength (true uniform strain)

In absence of the uniform strain data in available literature, it needs to be estimated based on stress-strains curves and elongation (strain corresponding to rupture of the tensile specimen).

The stress-strain curves for Alloy 22, 316 SS and 316NG SS do not manifest three-stage deformation characteristics (Ref. 12). Therefore, the elongation, reduced by 10% for the sake of conservatism (Assumption 3.8), can be used in place of uniform strain. 316 CS does manifest three-stage deformation, and will be reduced by 50% for the sake of conservatism (Assumption 3.9).

In the case of Alloy 22 ($e_u = 0.9 * \text{elongation} = 0.41$ at room temperature), the true measures of ductility are

$$\epsilon_u = \ln(1 + e_u) = \ln(1 + 0.41) = 0.34$$

$$\sigma_u = s_u * (1 + e_u) = 690 * (1 + 0.41) = 973 \text{ MPa}$$

400 °F (204 °C) Alloy 22

$$\epsilon_u = \ln(1 + e_u) = \ln(1 + 0.41) = 0.34$$

$$S_u = s_u * (1 + e_u) = 657 * (1 + 0.41) = 926 \text{ MPa}$$

600 °F (316 °C) Alloy 22

$$e_u = \ln(1 + e_u) = \ln(1 + 0.41) = 0.34 \quad (\text{ASME values})$$

$$S_u = s_u * (1 + e_u) = 628 * (1 + 0.41) = 885 \text{ MPa} \quad (\text{ASME values})$$

$$e_u = \ln(1 + e_u) = \ln(1 + 0.45) = 0.37 \quad (\text{vendor data})$$

$$S_u = s_u * (1 + e_u) = 628 * (1 + 0.45) = 911 \text{ MPa} \quad (\text{vendor data})$$

For 316NG SS at room temperature, $e_u = 0.9 * \text{elongation} = 0.36$, therefore:

$$e_u = \ln(1 + e_u) = \ln(1 + 0.36) = 0.31$$

$$S_u = s_u * (1 + e_u) = 517 * (1 + 0.36) = 703 \text{ MPa}$$

400 °F (204 °C) SS 316NG

$$e_u = \ln(1 + e_u) = \ln(1 + 0.36) = 0.31$$

$$S_u = s_u * (1 + e_u) = 496 * (1 + 0.36) = 675 \text{ MPa}$$

600 °F (316 °C) SS 316NG

$$e_u = \ln(1 + e_u) = \ln(1 + 0.36) = 0.31 \quad (\text{ASME values})$$

$$S_u = s_u * (1 + e_u) = 495 * (1 + 0.36) = 673 \text{ MPa} \quad (\text{ASME values})$$

600 °F (316 °C) SS 316NG(cont'd)

$$e_u = \ln(1 + e_u) = \ln(1 + 0.25) = 0.22 \quad (\text{vendor data})$$

$$S_u = s_u * (1 + e_u) = 495 * (1 + 0.25) = 619 \text{ MPa} \quad (\text{vendor data})$$

For 516 CS at room temperature, $e_u = 0.5 * \text{elongation} = 0.11$, therefore:

$$e_u = \ln(1 + e_u) = \ln(1 + 0.11) = 0.10$$

$$S_u = s_u * (1 + e_u) = 483 * (1 + 0.11) = 536 \text{ MPa}$$

400 °F (204 °C) 516 CS

$$e_u = \ln(1 + e_u) = \ln(1 + 0.11) = 0.10$$

$$S_u = s_u * (1 + e_u) = 483 * (1 + 0.11) = 536 \text{ MPa}$$

600 °F (316 °C) 516 CS

$$e_u = \ln(1 + e_u) = \ln(1 + 0.11) = 0.10$$

$$S_u = s_u * (1 + e_u) = 483 * (1 + 0.11) = 536 \text{ MPa}$$

For 304 SS at room temperature, $e_u = 0.75 * \text{elongation} = 0.30$, therefore:

$$e_u = \ln(1 + e_u) = \ln(1 + 0.30) = 0.26$$

$$S_u = s_u * (1 + e_u) = 517 * (1 + 0.30) = 672 \text{ MPa}$$

400 °F (204 °C) 304 SS

$$e_u = \ln(1 + e_u) = \ln(1 + 0.30) = 0.26$$

$$S_u = s_u * (1 + e_u) = 441 * (1 + 0.30) = 573 \text{ MPa}$$

600 °F (316 °C) 304 SS

$$e_u = \ln(1 + e_u) = \ln(1 + 0.30) = 0.26$$

$$s_u = s_u * (1 + e_u) = 437 * (1 + 0.30) = 568 \text{ MPa}$$

5.2.3 Calculations for Tangent Moduli

As previously discussed, the results of this simulation are required to include elastic and plastic deformations for Alloy 22, 516 CS, and 316NG SS. When the materials are driven into the plastic range, the slope of stress-strain curve continuously changes. Thus, a simplification for this curve is needed to incorporate plasticity into the FER. A standard approximation commonly used in engineering is to use a straight line that connects the yield point and the tensile strength point of the material. The parameters used in the subsequent calculations in addition to those defined in Section 5.2.2 are modulus of elasticity (E) and tangent modulus (E_t). The tangent (hardening) modulus represents the slope of the stress-strain curve in the plastic region.

In the case of Alloy 22, the strain corresponding to the yield strength is:

$$e_{y,rt} = s_y/E = 310 * 10^6 / 206 * 10^9 = 0.0015 \text{ (see Section 5.2.1)}$$

Hence, the tangent modulus at room temperature is:

$$E_{t,rt} = (s_{u,rt} - s_{y,rt}) / (e_{u,rt} - e_{y,rt}) = (0.973 - 0.310) / (0.34 - 0.0015) = 2.0 \text{ GPa} \text{ (see Section 5.2, 5.2.1, and 5.2.2)}$$

For Alloy 22 at 400 °F (204 °C)

$$E_{t,400°F} = (s_{u,400°F} - s_{y,400°F}) / (e_{u,400°F} - s_{y,400°F}/E_{400°F}) = (0.926 - 0.236) / (0.34 - 236/196e3) = 2.0 \text{ GPa} \text{ (see Section 5.2, 5.2.1, and 5.2.2)}$$

For Alloy 22 at 600 °F (316 °C, ASME values)

$$E_{t,600°F} = (s_{u,600°F} - s_{y,600°F}) / (e_{u,600°F} - s_{y,600°F}/E_{600°F}) = (0.885 - 0.211) / (0.34 - 211/190e3) = 2.0 \text{ GPa} \text{ (see Section 5.2, 5.2.1, and 5.2.2)}$$

For Alloy 22 at 600 °F (316 °C, vendor data)

$$E_{t,600°F} = (s_{u,600°F} - s_{y,600°F}) / (e_{u,600°F} - s_{y,600°F}/E_{600°F}) = (0.911 - 0.211) / (0.37 - 211/190e3) = 1.9 \text{ GPa} \text{ (see Section 5.2, 5.2.1, and 5.2.2)}$$

Similarly, for 316NG SS at room temperature:

$$E_{t,rt} = (s_{u,rt} - s_{y,rt}) / (e_{u,rt} - s_{y,rt}/E_{rt}) = (0.703 - 0.207) / (0.31 - 207/195e3) = 1.6 \text{ GPa} \text{ (see Section 5.2, 5.2.1, and 5.2.2)}$$

For 316NG SS at 400 °F (204 °C)

$$E_{t,400°F} = (s_{u,400°F} - s_{y,400°F}) / (e_{u,400°F} - s_{y,400°F}/E_{400°F}) = (0.675 - 0.148) / (0.31 - 148/183e3) = 1.7 \text{ GPa} \text{ (see Section 5.2, 5.2.1, and 5.2.2)}$$

For 316NG SS at 600 °F (316 °C, ASME values)

$$E_{I,600^{\circ}F} = (\mathbf{S}_{u,600^{\circ}F} - \mathbf{S}_{y,600^{\circ}F}) / (\mathbf{e}_{u,600^{\circ}F} - \mathbf{S}_{y,600^{\circ}F}/E_{600^{\circ}F}) = (0.673 - 0.130)/(0.31 - 130/174e3) = 1.8 \text{ GPa} \text{ (see Section 5.2, 5.2.1, and 5.2.2)}$$

For 316NG SS at 600 °F (316 °C, vendor data)

$$E_{I,600^{\circ}F} = (\mathbf{S}_{u,600^{\circ}F} - \mathbf{S}_{y,600^{\circ}F}) / (\mathbf{e}_{u,600^{\circ}F} - \mathbf{S}_{y,600^{\circ}F}/E_{600^{\circ}F}) = (0.619 - 0.130)/(0.22 - 130/174e3) = 2.2 \text{ GPa} \text{ (see Section 5.2, 5.2.1, and 5.2.2)}$$

Tangent Modulus of 516 CS at room temperature:

$$E_{I,rt} = (\mathbf{S}_{u,rt} - \mathbf{S}_{y,rt}) / (\mathbf{e}_{u,rt} - \mathbf{S}_{y,rt}/E_{rt}) = (0.536 - 0.262)/(0.10 - 262/203e3) = 2.8 \text{ GPa} \text{ (see Section 5.2, 5.2.1, and 5.2.2)}$$

516 CS at 400 °F (204 °C)

$$E_{I,400^{\circ}F} = (\mathbf{S}_{u,400^{\circ}F} - \mathbf{S}_{y,400^{\circ}F}) / (\mathbf{e}_{u,400^{\circ}F} - \mathbf{S}_{y,400^{\circ}F}/E_{400^{\circ}F}) = (0.536 - 0.224)/(0.10 - 224/191e3) = 3.2 \text{ GPa} \text{ (see Section 5.2, 5.2.1, and 5.2.2)}$$

516 CS at 600 °F (316 °C)

$$E_{I,600^{\circ}F} = (\mathbf{S}_{u,600^{\circ}F} - \mathbf{S}_{y,600^{\circ}F}) / (\mathbf{e}_{u,600^{\circ}F} - \mathbf{S}_{y,600^{\circ}F}/E_{600^{\circ}F}) = (0.536 - 0.201)/(0.10 - 201/184e3) = 3.4 \text{ GPa} \text{ (see Section 5.2, 5.2.1, and 5.2.2)}$$

Tangent Modulus of 304 SS at room temperature:

$$E_{I,rt} = (\mathbf{S}_{u,rt} - \mathbf{S}_{y,rt}) / (\mathbf{e}_{u,rt} - \mathbf{S}_{y,rt}/E_{rt}) = (0.672 - 0.207)/(0.26 - 207/195e3) = 1.8 \text{ GPa} \text{ (see Section 5.2, 5.2.1, and 5.2.2)}$$

304 SS at 400 °F (204 °C)

$$E_{I,400^{\circ}F} = (\mathbf{S}_{u,400^{\circ}F} - \mathbf{S}_{y,400^{\circ}F}) / (\mathbf{e}_{u,400^{\circ}F} - \mathbf{S}_{y,400^{\circ}F}/E_{400^{\circ}F}) = (0.573 - 0.143)/(0.26 - 143/183e3) = 1.7 \text{ GPa} \text{ (see Section 5.2, 5.2.1, and 5.2.2)}$$

304 SS at 600 °F (316 °C)

$$E_{I,600^{\circ}F} = (\mathbf{S}_{u,600^{\circ}F} - \mathbf{S}_{y,600^{\circ}F}) / (\mathbf{e}_{u,600^{\circ}F} - \mathbf{S}_{y,600^{\circ}F}/E_{600^{\circ}F}) = (0.568 - 0.127)/(0.26 - 127/174e3) = 1.7 \text{ GPa} \text{ (see Section 5.2, 5.2.1, and 5.2.2)}$$

5.3 INITIAL VELOCITY OF WASTE PACKAGE

To reduce the computer execution time while preserving all features of the problem relevant to the structural calculation, the WP is set in a position just before impact and given an appropriate initial velocity, as can be seen in Figure 1.

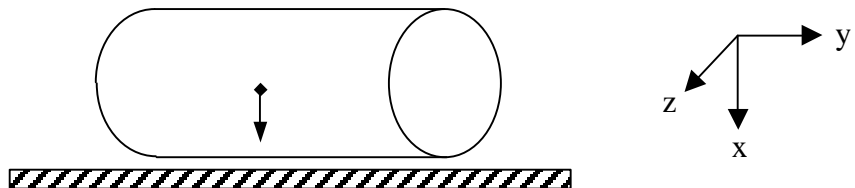


Figure 1. Horizontal Drop Geometry

Using the following parameters:

$$g \equiv \text{acceleration due to gravity} = 9.81 \text{ m/s}^2$$

$$S \equiv \text{Drop Height} = 2.4 \text{ m} \text{ (Ref. 1)}$$

and Newton's equation of motion:

$$V^2 = V_o^2 + 2a(S - S_o)$$

Substituting values in yields

$$V^2 = 0^2 + 2*(9.81 \text{ m/s}^2)*(2.4 \text{ m}), \text{ which reduces to}$$

$$V = 6.86 \text{ m/s}$$

5.4 FINITE ELEMENT REPRESENTATION

A full three-dimensional (3-D) FER of the WP was developed in ANSYS V5.4 using the dimensions provided in Attachment I. The FER was created with a radial gap of 5 mm between the inner and outer shells. The same gap was used between the internals and the inner shell. The initial orientation of the inner shell maintains a 5 mm gap around the circumference of the shell.

The internal structure of the WP was simplified. The fuel assemblies of the IS were represented using solid elements as 21 separate rectangles. The thermal shunts, fuel tubes, and dividing plates were omitted. The spent fuel density was increased to account for the missing mass. But, the sideguides, conerguides, and stiffeners were included (Assumption 3.5). This method of representing the contact between the internals and the IS is more accurate than previously used in Revision 00.

The target surface was conservatively assumed to be unyielding (Assumption 3.7). This was accomplished using the *RIGIDWALL command within LS-DYNA. This command creates an invisible rigid wall within LS-DYNA. All nodes are slaves to the RIGIDWALL, and the RIGIDWALL is immovable.

The mesh of the FER was appropriately generated and refined in the contact region according to standard engineering practice. Thus, the accuracy of the results of this calculation is deemed acceptable.

The initial drop height of the WP was reduced to 0.01 m before impact and the WP was given an initial velocity equal to 6.86 m/s (see Section 5.3).

The FER was then used in LS-DYNA V950.C to perform the transient dynamic analysis for the 21-PWR Waste Package horizontal drop.

6. RESULTS

This document may be affected by technical product input information that requires confirmation. Any changes to the document that may occur as a result of completing the confirmation activities will be reflected in subsequent revisions. The status of the technical product input information quality may be confirmed by review of the DIRS database.

| Attachment II includes the input files and results files that show execution of the programs occurred correctly. The stresses were reported via plots that have been made interactively using the postprocessor LSPOST. The stresses were recorded every 0.001 seconds after impact. The stresses in all components peaked between 0.004 and 0.017 seconds. However, the solution was allowed to reach 0.021 seconds to ensure that all stresses had climaxed.

| The results file, d3hsp (Attachment II), lists the calculated masses used by LS-DYNA. The sum of the masses of the WP equals 42,550 kg, with the mass of the loaded WP 41,598 kg from Section 5.1. The percent difference in mass would then be ~ 2.3%. However, this difference is on the positive side, and thus considered to be conservative and negligible.

| The following pages contain figures that show various parts at states of maximum stress. These start on the next page with Figure 2, which shows the maximum stress in the lower trunnion collar at room temperature.

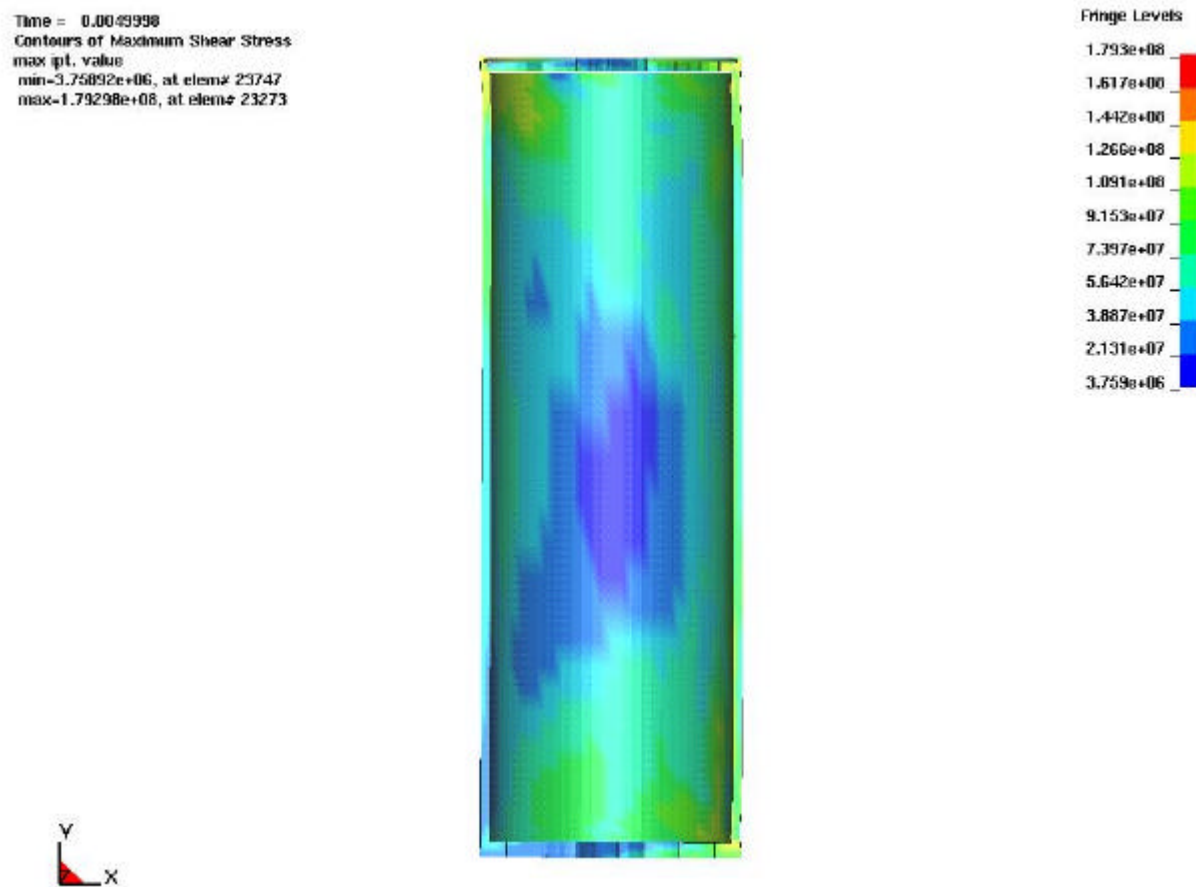


Figure 2. Inner Shell Stresses at Room Temperature

All of the stresses that are reported in the legends of the plots are Tresca Stresses or Maximum Shear Stresses. The units are Pascals. Figure 2 shows that the maximum stress intensity in the IS is 359 MPa at 0.005 seconds.

Figure 3 may be found on the next page. It shows the maximum stress in the same part, but at 400 degrees Fahrenheit.

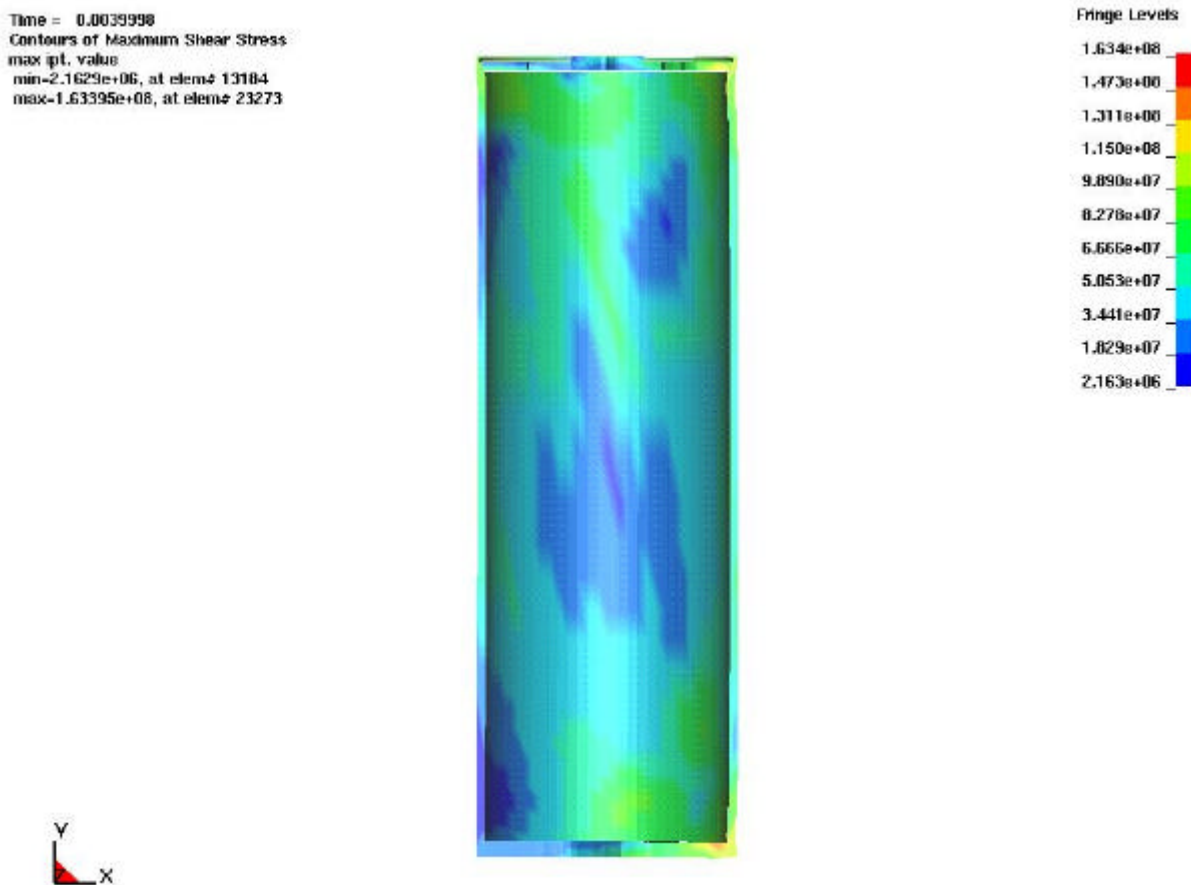


Figure 3. Inner Shell Stresses at 400 °F

Figure 3 shows that the maximum stress intensity in the IS is 327 MPa at 0.004 seconds. This is slightly lower than the room temperature value, which is to be expected.

Figure 4 may be found on the next page. It shows the maximum stress in the same part, but at 600 degrees Fahrenheit.

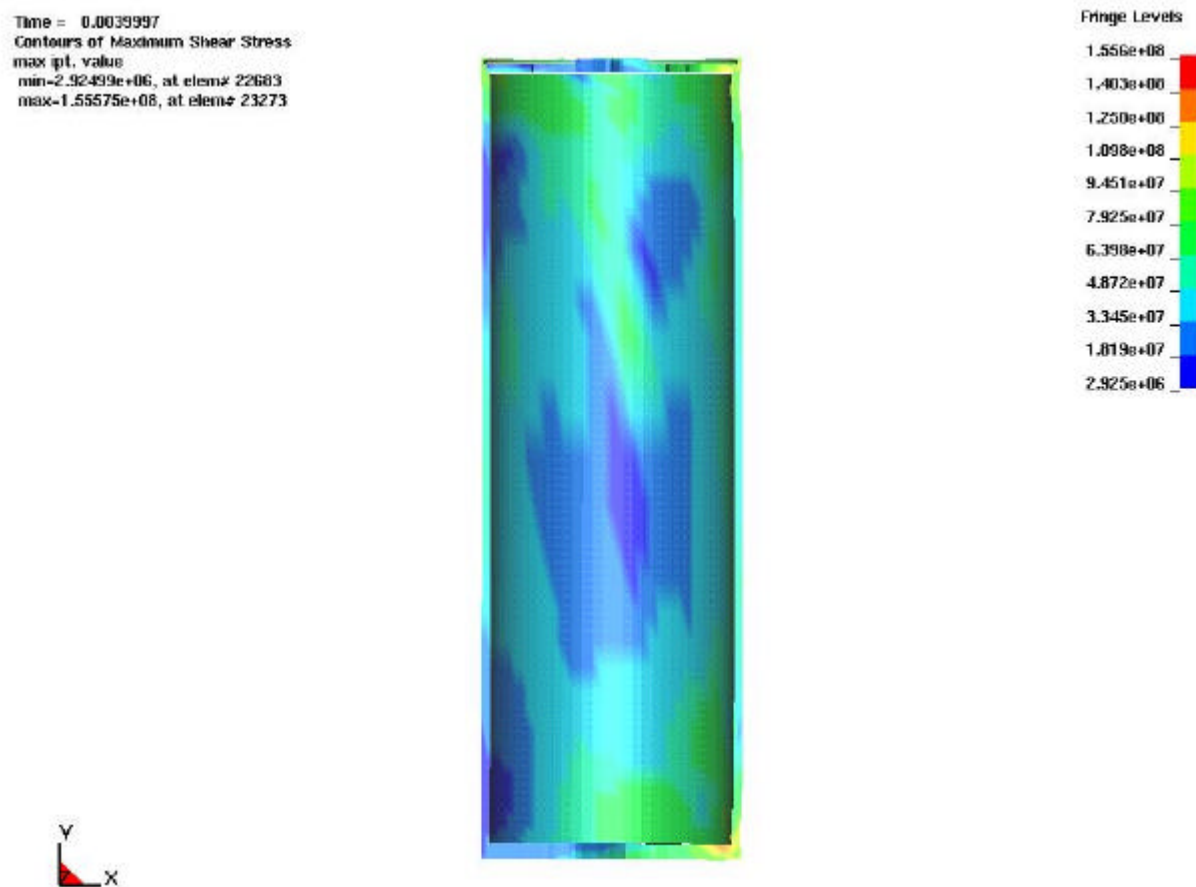


Figure 4. Inner Shell Stresses at 600 °F

Figure 4 shows that the maximum stress intensity in the IS is 311 MPa at 0.004 seconds. This is slightly lower than the 400 °F value, which is to be expected.

Figure 5 may be found on the next page. It shows the maximum stress in the Inner Shell at 600 degrees Fahrenheit, but using vendor data for the elongation values.

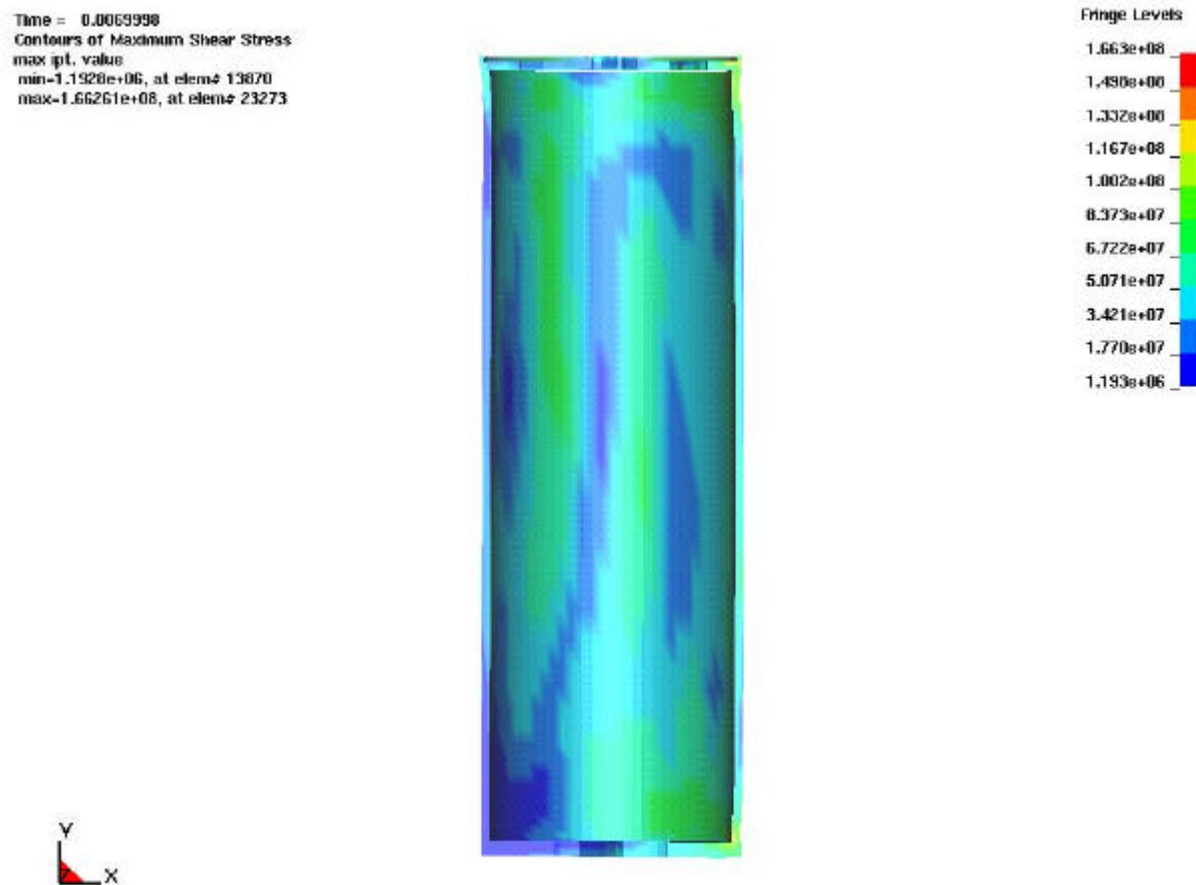


Figure 5. Inner Shell Stresses at 600 °F Using Vendor Elongation Values

Figure 5 shows that the maximum stress intensity in the IS is 333 MPa at 0.007 seconds. This is slightly higher than that shown in Figure 4, which is to be expected due to the elongation values of 316NG SS at elevated temperatures.

Figure 6 may be found on the next page. It shows the maximum stress in the outer shell at room temperature.

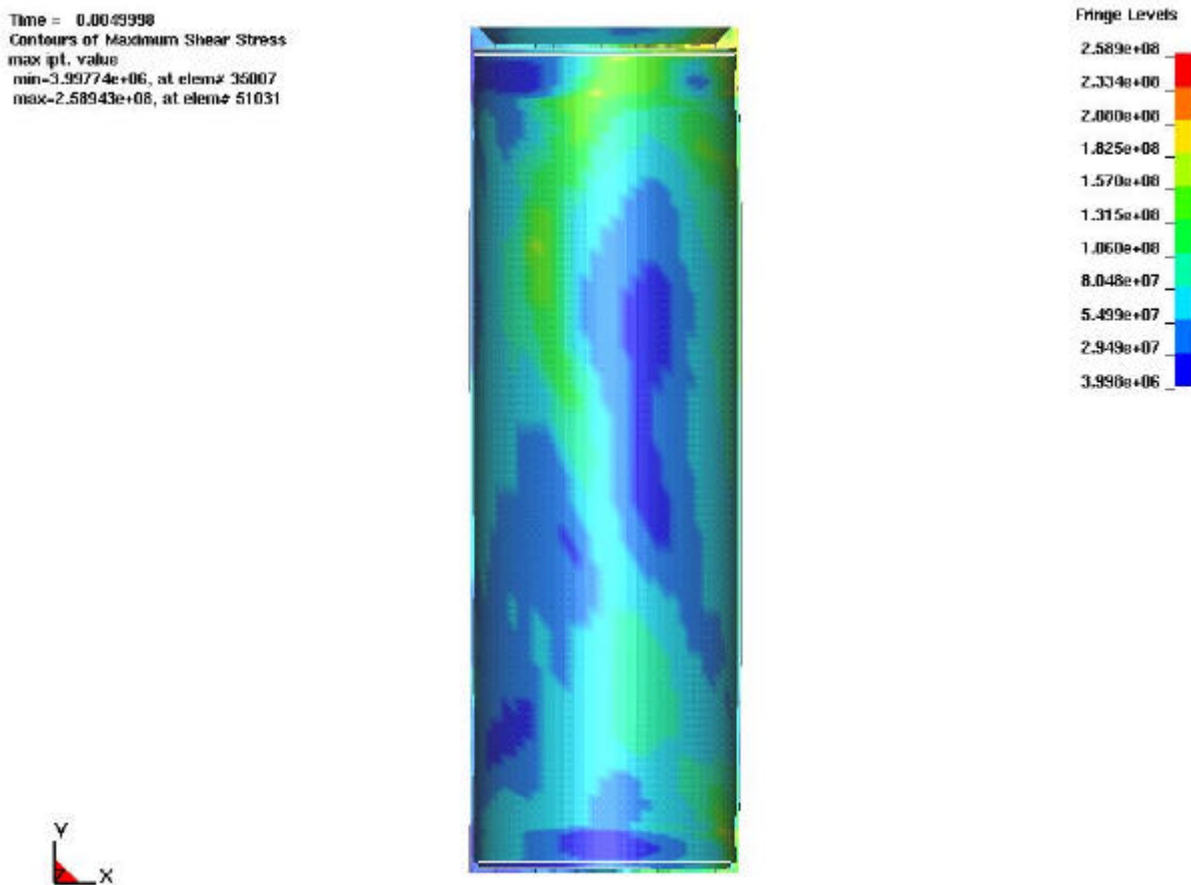


Figure 6. Outer Shell Maximum Stresses at Room Temperature

Figure 6 shows that the maximum stress intensity in the OS is 518 MPa at 0.005 seconds.

Figure 7 may be found on the next page. It shows the maximum stress in the same part, but at 400 degrees Fahrenheit.

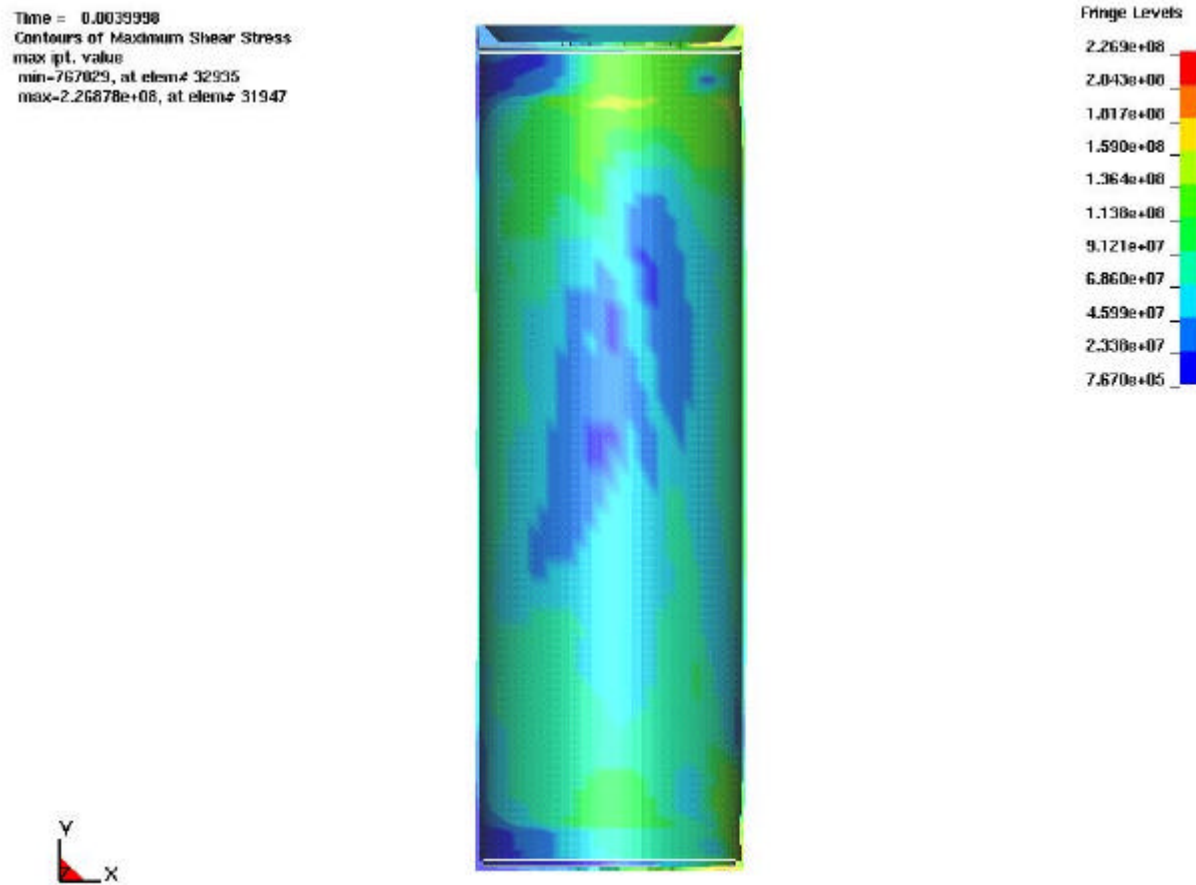


Figure 7. Outer Shell Maximum Stresses at 400 °F

Figure 7 shows that the maximum stress intensity in the OS is 454 MPa at 0.004 seconds. This is slightly lower than the 400 °F value, which is to be expected.

Figure 8 may be found on the next page. It shows the maximum stress in the OS at 600 degrees Farenheit.

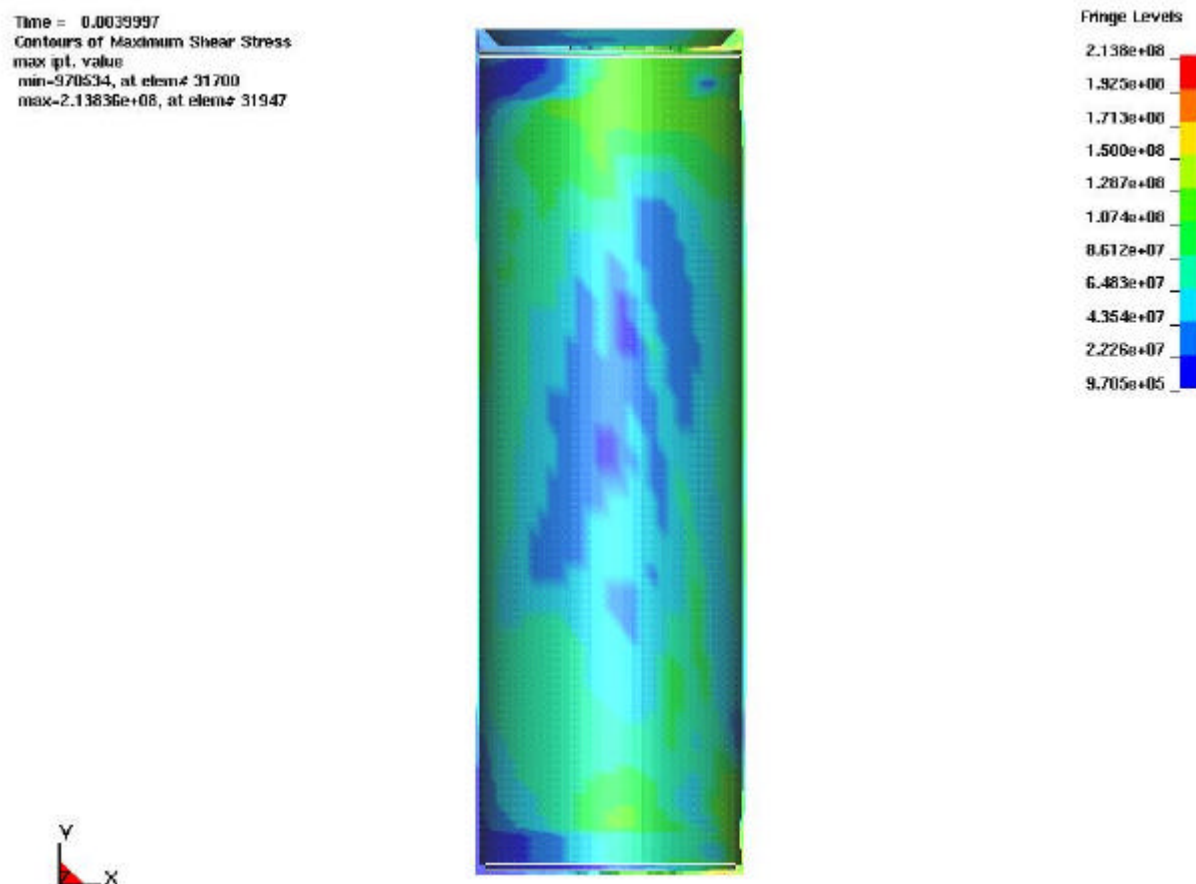


Figure 8. Outer Shell Maximum Stresses at 600 °F

Figure 8 shows that the maximum stress intensity in the OS is 428 MPa at 0.004 seconds. This is slightly lower than the 400 °F value, which is expected.

Figure 9 may be found on the next page. It shows the maximum stress in the same part and at the same temperature, but using vendor data for the elongation values.

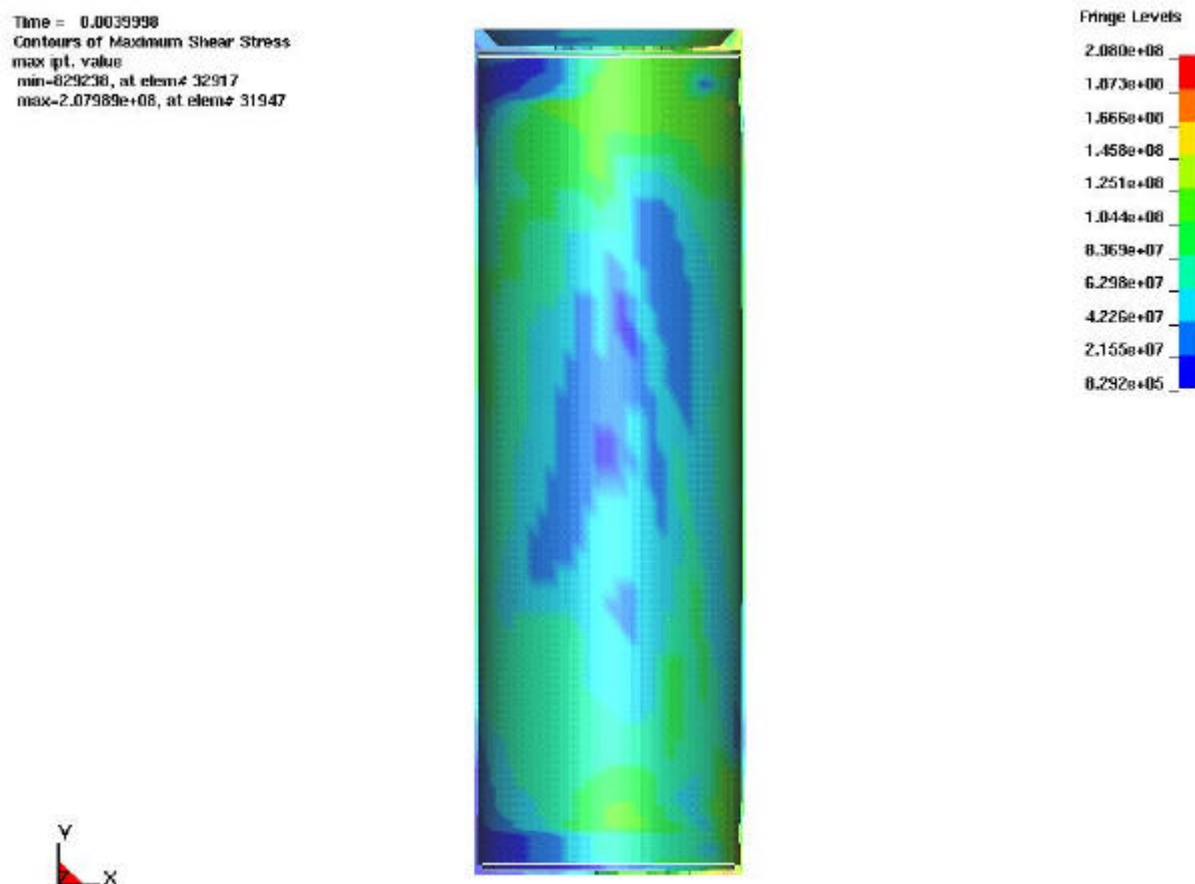


Figure 9. Outer Shell Maximum Stresses at 600 °F Using Vendor Elongation

Figure 9 shows that the maximum stress intensity in the OS is 416 MPa at 0.004 seconds. This is slightly higher than shown in Figure 8, which is to be expected due to Alloy 22 elongation properties at elevated temperatures.

Figure 10 may be found on the next page. It shows the maximum stress in the Shear Ring at room temperature.

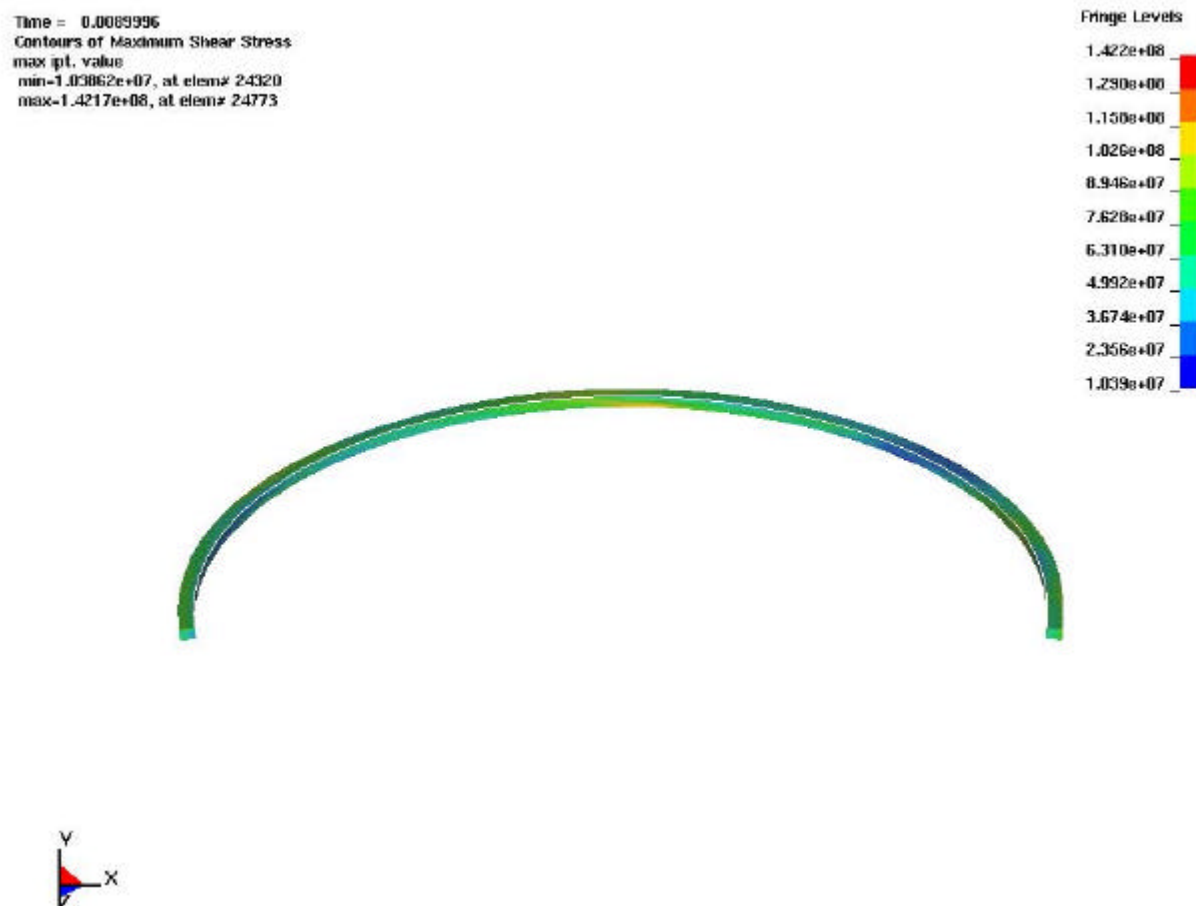


Figure 10. Shear Ring Maximum Stresses at Room Temperature

Figure 10 shows that the maximum stress intensity in the Shear Ring is 284 MPa at 0.009 seconds.

Figure 11 may be found on the next page. It shows the maximum stress in the Shear Ring at 400 degrees Fahrenheit.



Figure 11. Shear Ring Maximum Stresses at 400 °F

Figure 11 shows that the maximum stress intensity in the Shear Ring is 211 MPa at 0.010 seconds. This is lower than the room temperature value, which is to be expected.

Figure 12 may be found on the next page. It shows the maximum stress in the Shear Ring at 600 degrees Fahrenheit.

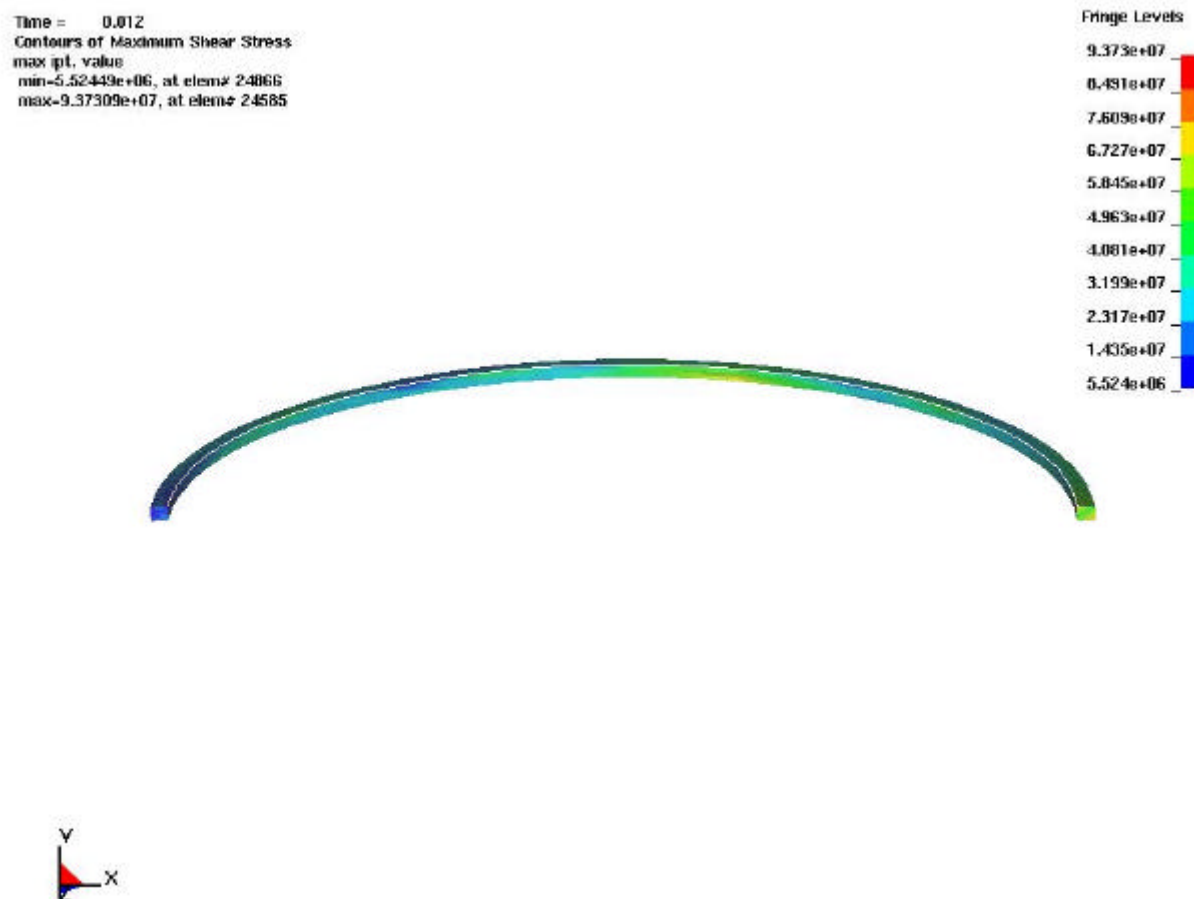


Figure 12. Shear Ring Maximum Stresses at 600 °F

Figure 12 shows that the maximum stress intensity in the Shear Ring is 187 MPa at 0.012 seconds. This is slightly higher than the 400 °F value, which is to be expected.

Figure 13 may be found on the next page. It shows the maximum stress in the Shear Ring at the same temperature, but using vendor data elongation values.

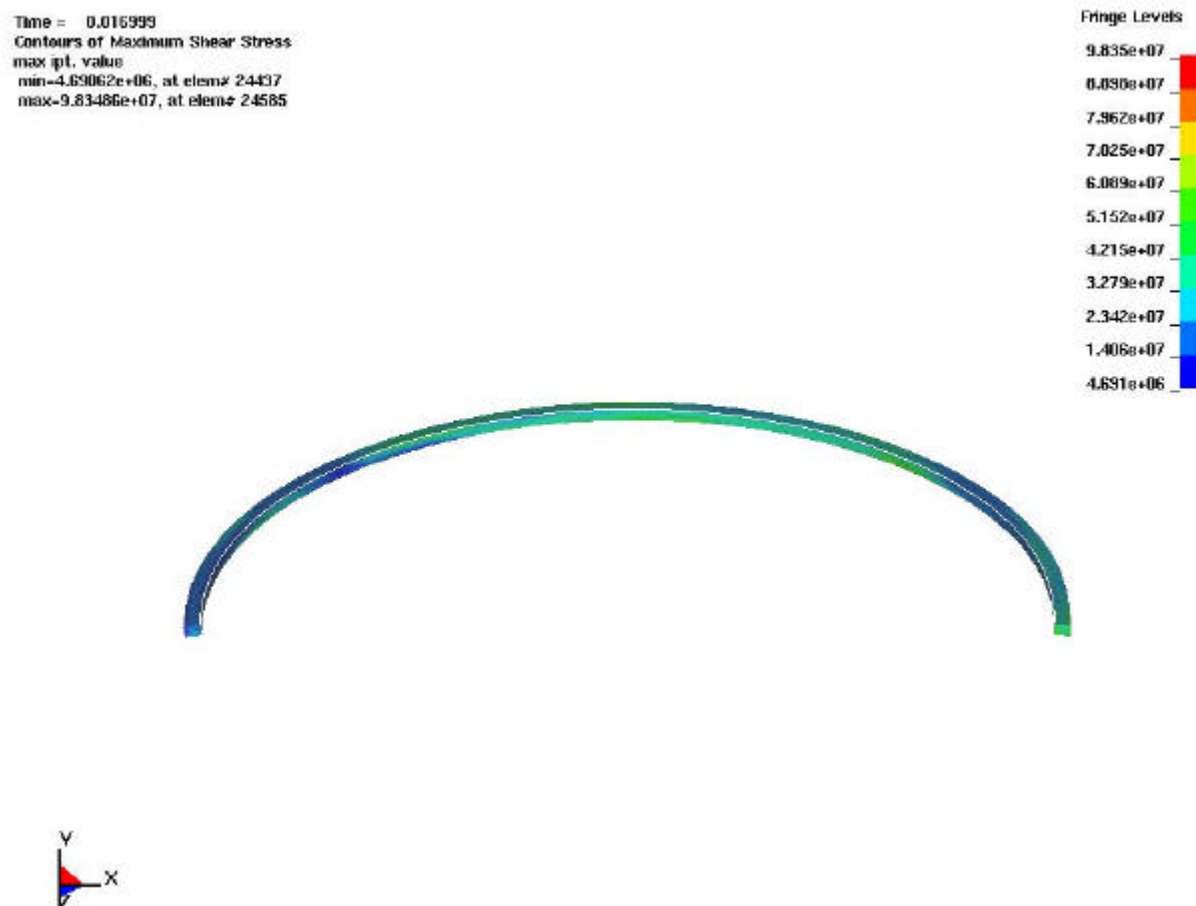


Figure 13. Shear Ring Maximum Stresses at 600 °F Using Vendor Elongation

Figure 13 shows that the maximum stress intensity in the Shear Ring is 197 MPa at 0.017 seconds. This is slightly higher than that shown in Figure 12, which is expected due to 316NG SS elongation properties at elevated temperatures.

Table 6-1 summarizes the maximum Stress Intensities, sorted by Part, Temperature, and Elongation Value per Load Case.

Table 6-1. Maximum Stress Intensity by Load Case

Part	Temperature	Elongation Value	Max Stress Intensity	$S_{int} / S_{allowable}$
Inner Shell	70 °F	ASME	359 MPa	0.567
Outer Shell	70 °F	ASME	518 MPa	0.592
Shear Ring	70 °F	ASME	284 MPa	0.449
Inner Shell	400 °F	ASME	327 MPa	0.538
Outer Shell	400 °F	ASME	454 MPa	0.545
Shear Ring	400 °F	ASME	211 MPa	0.347
Inner Shell	600 °F	ASME	311 MPa	0.513
Outer Shell	600 °F	ASME	428 MPa	0.537
Shear Ring	600 °F	ASME	187 MPa	0.309
Inner Shell	600 °F	ASME - 30%	333 MPa	0.598
Outer Shell	600 °F	ASME + 10%	416 MPa	0.507
Shear Ring	600 °F	ASME - 30%	197 MPa	0.354

Note: $S_{allowable}$ is equal to 90% of σ_u .

7. REFERENCES

1. CRWMS M&O 2000. *Uncanistered Spent Nuclear Fuel Disposal Container System Description Document*. SDD-UDC-SE-000001 REV 01. Las Vegas, Nevada: CRWMS M&O. ACC: MOL.20000822.0004.
2. ASME (American Society of Mechanical Engineers) 1998. *1998 ASME Boiler and Pressure Vessel Code*. 1998 Edition, Including Addenda. New York, New York: American Society of Mechanical Engineers. TIC: 247429.
3. ASM International 1990. *Properties and Selection: Irons, Steels, and High-Performance Alloys*. Volume 1 of *Metals Handbook*. 10th Edition. Materials Park, Ohio: ASM International. TIC: 245666.
4. CRWMS M&O 2000. *Software Code: ANSYS*. V5.6.2. HP-UX 10.20. 10364-5.6.2-00.
5. Bowles, J.E. 1980. *Structural Steel Design*. New York, New York: McGraw-Hill. TIC: 249182.
6. Haynes International 1997. *Hastelloy C-22 Alloy*. Kokomo, Indiana: Haynes International. TIC: 238121.
7. CRWMS M&O 2000. *Software Code: LS-DYNA*. V950. HP 9000. 10300-950-00. URN-0368
8. Boyer, H.E., ed. 2000. *Atlas of Stress-Strain Curves*. Metals Park, Ohio: ASM International. TIC: 248901.
9. Not used.
10. AP-SV.1Q, Rev. 0, ICN 2. *Control of the Electronic Management of Information*. Washington, D.C.: U.S. Department of Energy, Office of Civilian Radioactive Waste Management. ACC: MOL. 20000831.0065.
11. AP-3.12Q, Rev. 0, ICN 4. *Calculations*. Washington, D.C.: U.S. Department of Energy, Office of Civilian Radioactive Waste Management. ACC: MOL.20010404.0008.
12. CRWMS M&O 2000. *Stress-Strain-Curve character for Alloy 22 and 316 Stainless Steel*. Input Transmittal 00384.T. Las Vegas, Nevada: CRWMS M&O. ACC: MOL.20001013.0053.
13. ASM (American Society for Metals) 1980. *Properties and Selection: Stainless Steels, Tool Materials and Special-Purpose Metals*. Volume 3 of *Metals Handbook*. 9th Edition. Metals Park, Ohio: American Society for Metals. TIC: 209801.

14. ASTM G 1-90 (Reapproved 1999). 1990. *Standard Practice for Preparing, Cleaning, and Evaluating Corrosion Test Specimens*. West Conshohocken, Pennsylvania: American Society for Testing and Materials. TIC: 238771.
15. Dieter, G.E. 1976. *Mechanical Metallurgy*. 2nd Edition. Materials Science and Engineering Series. New York, New York: McGraw-Hill Book Company. TIC: 247879.
16. CRWMS M&O 2000. *Technical Work Plan for: Waste Package Design Description for LA*. TWP-EBS-MD-000004 REV 00. Las Vegas, Nevada: CRWMS M&O. ACC: MOL.20001107.0304.
17. Allegheny Ludlum. 1987. Technical Data Blue Sheet for Stainless Steels Chromium-Nickel-Molybdenum, Types 316, 316L, 317, and 317L. Pittsburgh, Pennsylvania: Allegheny Ludlum Corporation. TIC: 240370.
18. ASM International 1987. *Corrosion*. Volume 13 of Metals Handbook. 9th Edition. Metals Park, Ohio: ASM International. TIC: 209807.
19. CRWMS M&O 1997. *Waste Container Cavity Size Determination*. BBAA00000-01717-0200-00026 REV 00. Las Vegas, Nevada: CRWMS M&O. ACC: MOL.19980106.0061.

8. ATTACHMENTS

Attachment I (25 pages): Design sketch (*21-PWR Waste Package Concept for License Application* [SK-0219 REV 01, 25 sheets])

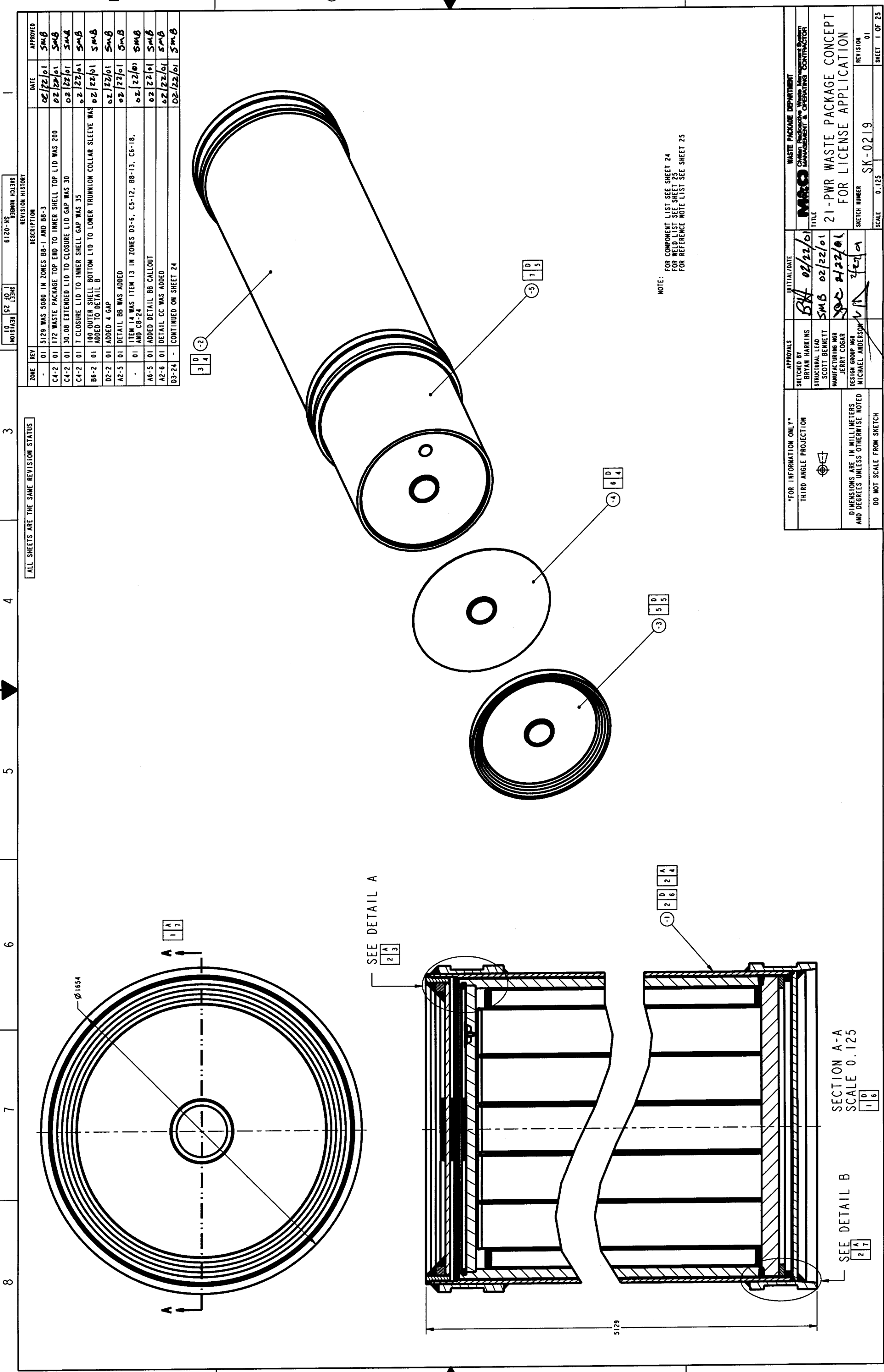
Attachment II (on compact disc): contains electronic files (see Table 8-1 for a complete list). The *.k files are input files for LS-DYNA at the three temperatures and they call the *.inc files. The d3hsp files are the LS-DYNA output files at the three temperatures.

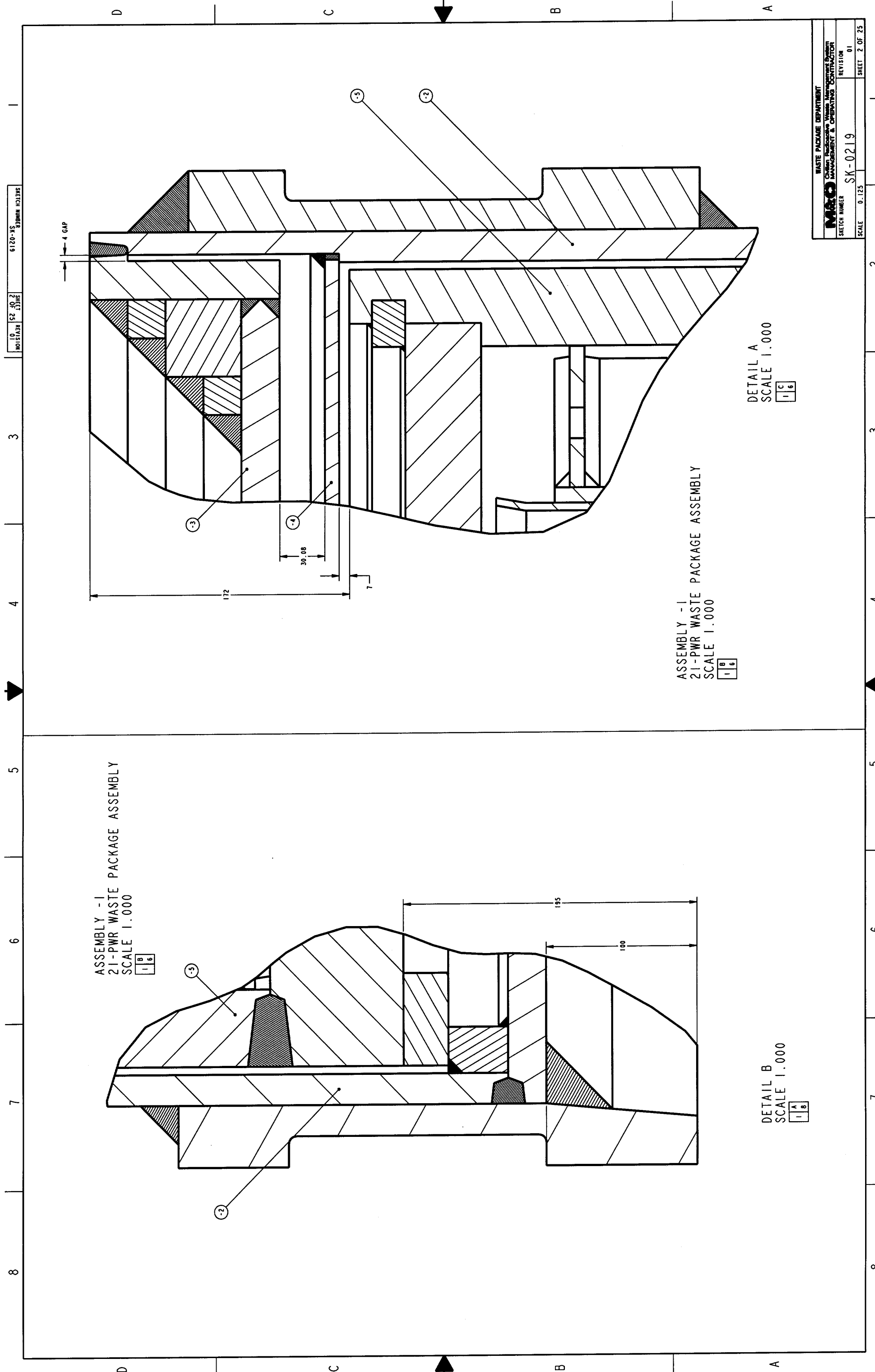
Table 8-1 provides a list of attachments submitted in the form of electronic files (compact disc) in Attachment II.

Table 8-1. List of Attachments Submitted in the Form of Electronic Files in Attachment II

Description	Date	Time	Size
d3hspt1	01/31/2001	1:44 pm	26,341 KB
d3hspt2	01/31/2001	1:49 pm	26,332 KB
d3hspt3	01/31/2001	1:51 pm	26,327 KB
d3hspt3v	01/31/2001	1:47 pm	26,327 KB
elist.inc	01/31/2001	1:44 pm	5,439 KB
hdsr.inp	01/31/2001	1:45 pm	37 KB
hdt1.k	01/31/2001	1:44 pm	3 KB
hdt2.k	01/31/2001	1:49 pm	3 KB
hdt3.k	01/31/2001	1:51 pm	3 KB
hdt3v.k	01/31/2001	1:47 pm	3 KB
nlist.inc	01/31/2001	1:45 pm	5,563 KB

NOTE: The file sizes may vary with operating system.





ASSEMBLY -2
OUTER SHELL ASSEMBLY
SCALE 0.150

A diagram of a 6x6 Rubik's cube. The cube is shown in a partially solved state with various faces labeled. The faces are labeled as follows: Top face (T) has '17 1' in the top-left corner; Middle face (M) has '16 2' in the top-left corner; Right face (R) has '16 4' in the top-left corner; Bottom face (B) has '15 8' in the top-left corner; Left face (L) has '15 6' in the top-left corner; and Front face (F) has '14 2' in the top-left corner. Arrows indicate moves: an arrow from the '17 1' label points to the top-left corner of the top face; an arrow from the '16 2' label points to the top-left corner of the middle face; an arrow from the '16 4' label points to the top-left corner of the right face; an arrow from the '15 8' label points to the top-left corner of the bottom face; an arrow from the '15 6' label points to the top-left corner of the left face; and an arrow from the '14 2' label points to the top-left corner of the front face. The cube's faces are represented by concentric circles.

A technical drawing of a circular component. The outermost boundary is a thick black line. Inside it, there are two concentric circles, both represented by thin black lines. A horizontal dashed line passes through the center of the circles. A vertical dashed line is also present, intersecting the horizontal line at the center. A dimension line with arrows at the top left indicates a diameter of $\phi 1654$. At the top center, there is a small rectangular callout containing the text 'A 3 8' and a horizontal arrow pointing to the right. At the bottom center, there is another small rectangular callout containing the text 'B' and a horizontal arrow pointing to the right.

SEE DETAIL C -

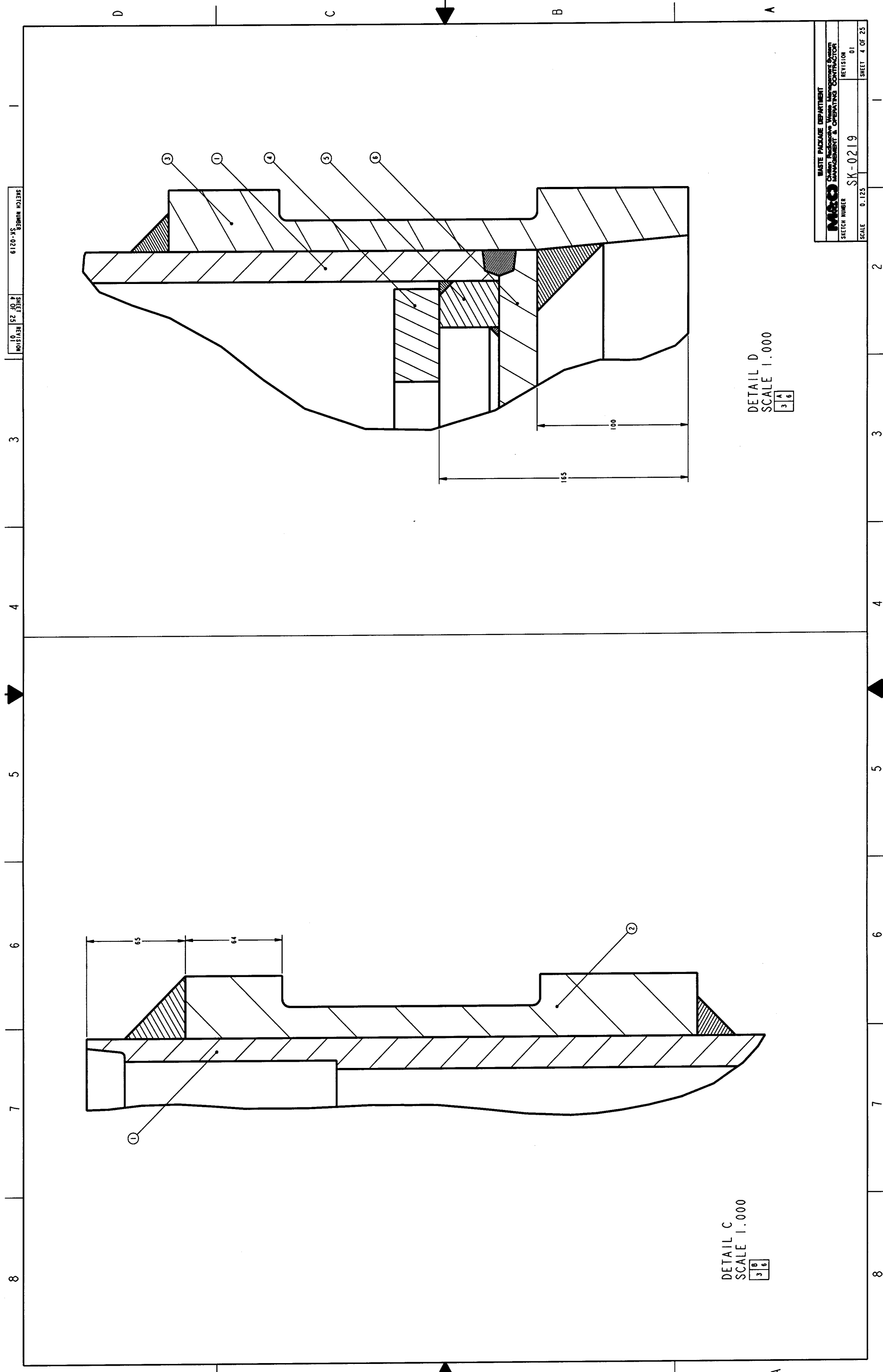
A vertical cylindrical container is shown. The base and the top lid are hatched with diagonal lines. The body of the cylinder is white. A horizontal dashed line is drawn across the middle of the cylinder, intersecting the hatched base and top.

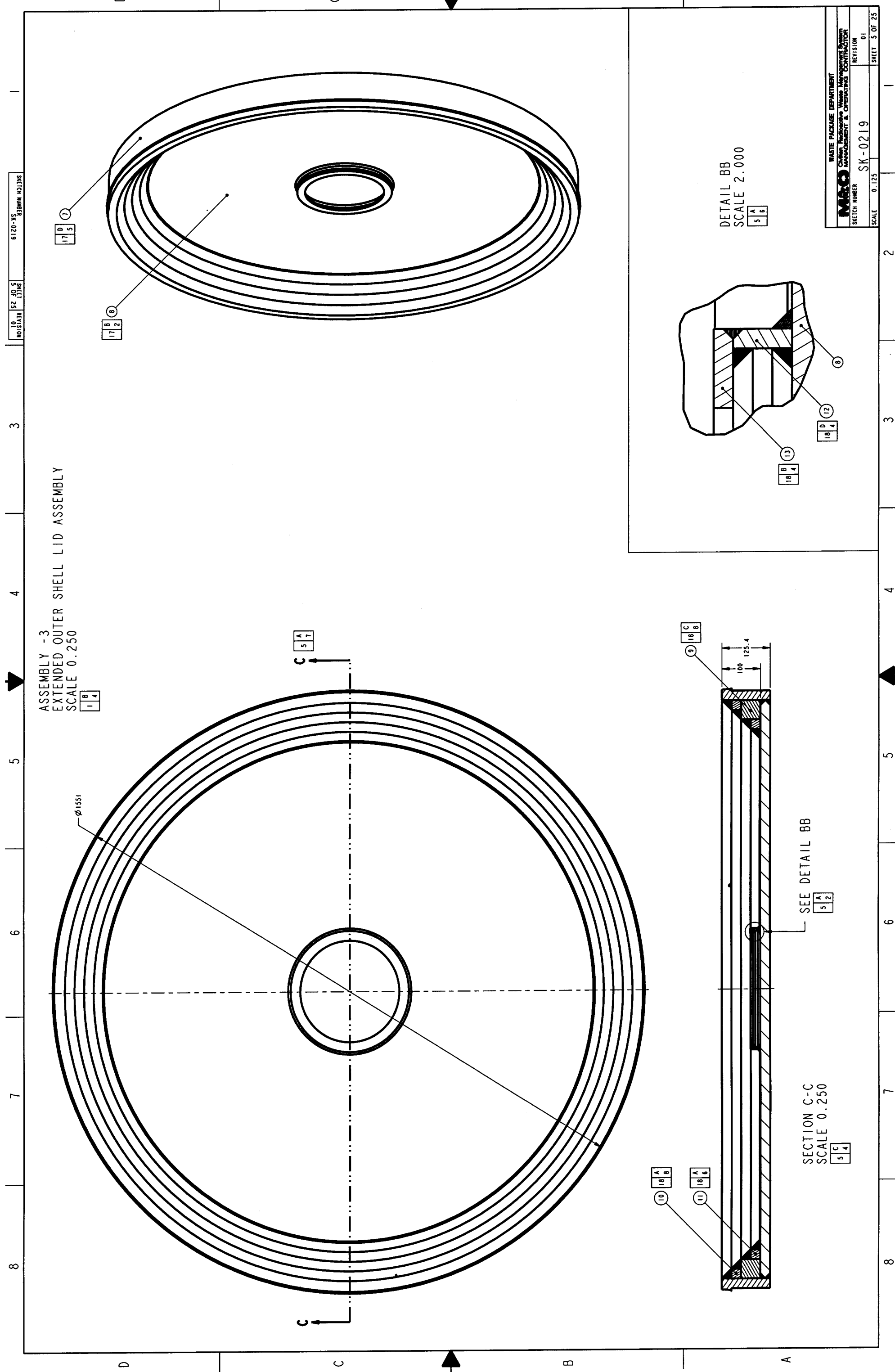
A technical cross-section diagram of a vertical pipe assembly. The pipe is shown in perspective, with a vertical dashed line representing the central axis. The pipe is supported by a bracket at the bottom and a flange at the top. The interior of the pipe is divided into three sections by two vertical partitions. The leftmost section is solid, the middle section is hatched with diagonal lines, and the rightmost section is hatched with vertical lines. The top of the pipe is open, and the interior is shown with a cross-hatched pattern. A small circular inset at the top right shows a magnified view of the top flange area.

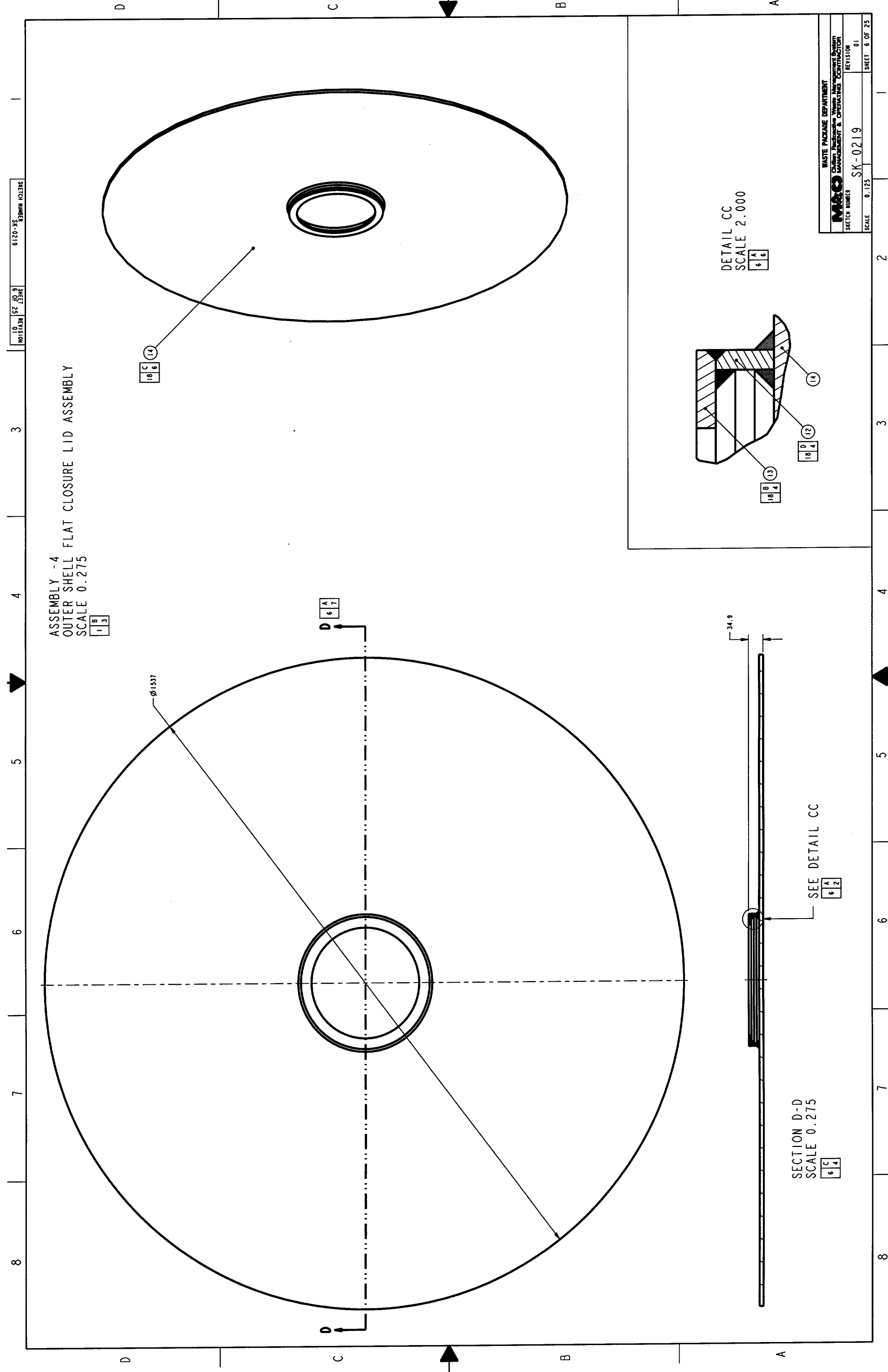
SECTION B-B
SCALE 0.150

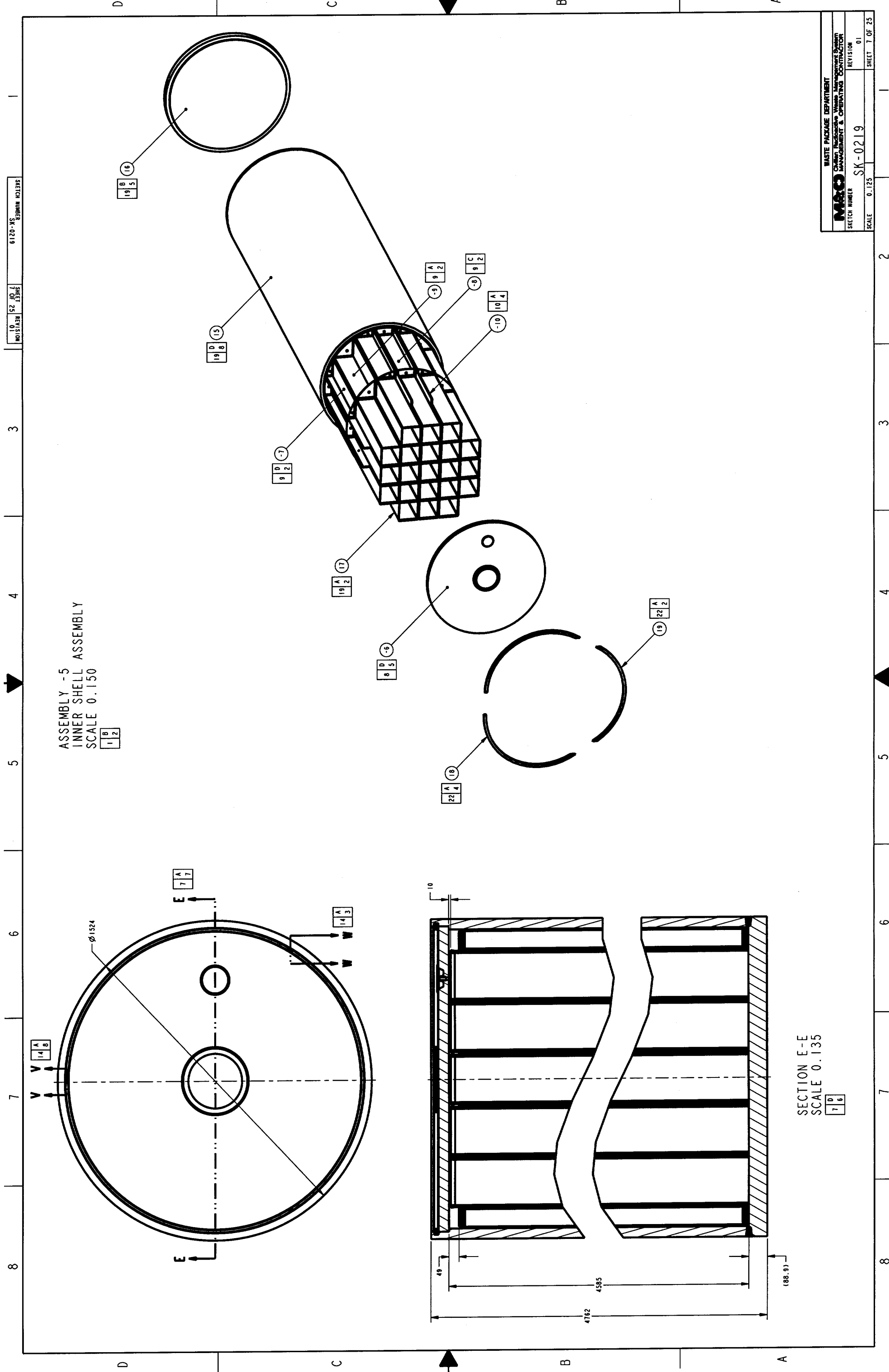
SEE DETAIL D -

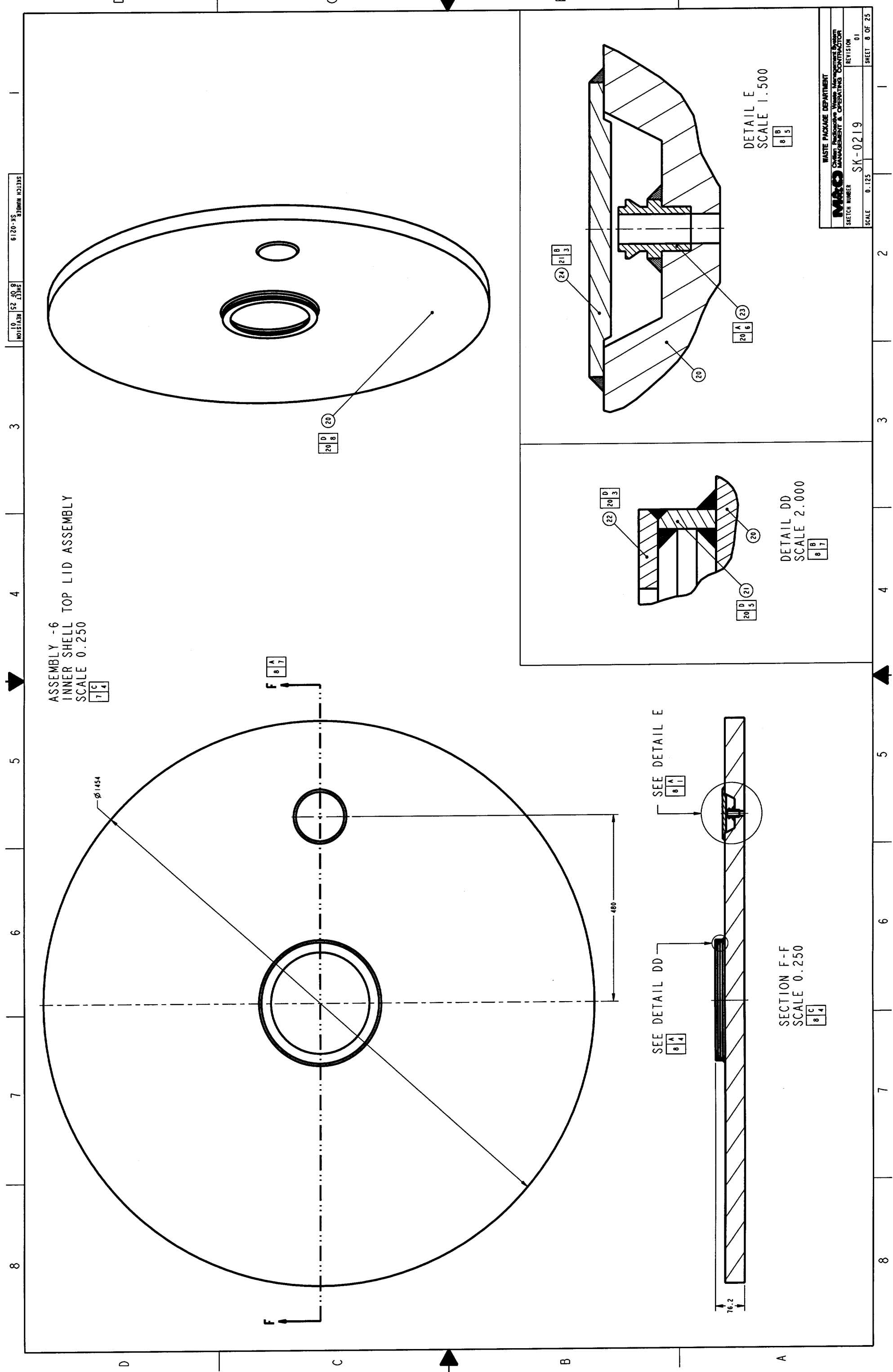
WASTE PACKAGE DEPARTMENT	
WACO <small>Chemical Processing</small> <small>Waste Management System</small> WASTE MANAGEMENT & OPERATING CONTRACTOR	
SKETCH NUMBER	SK - 0219
REVISION	01

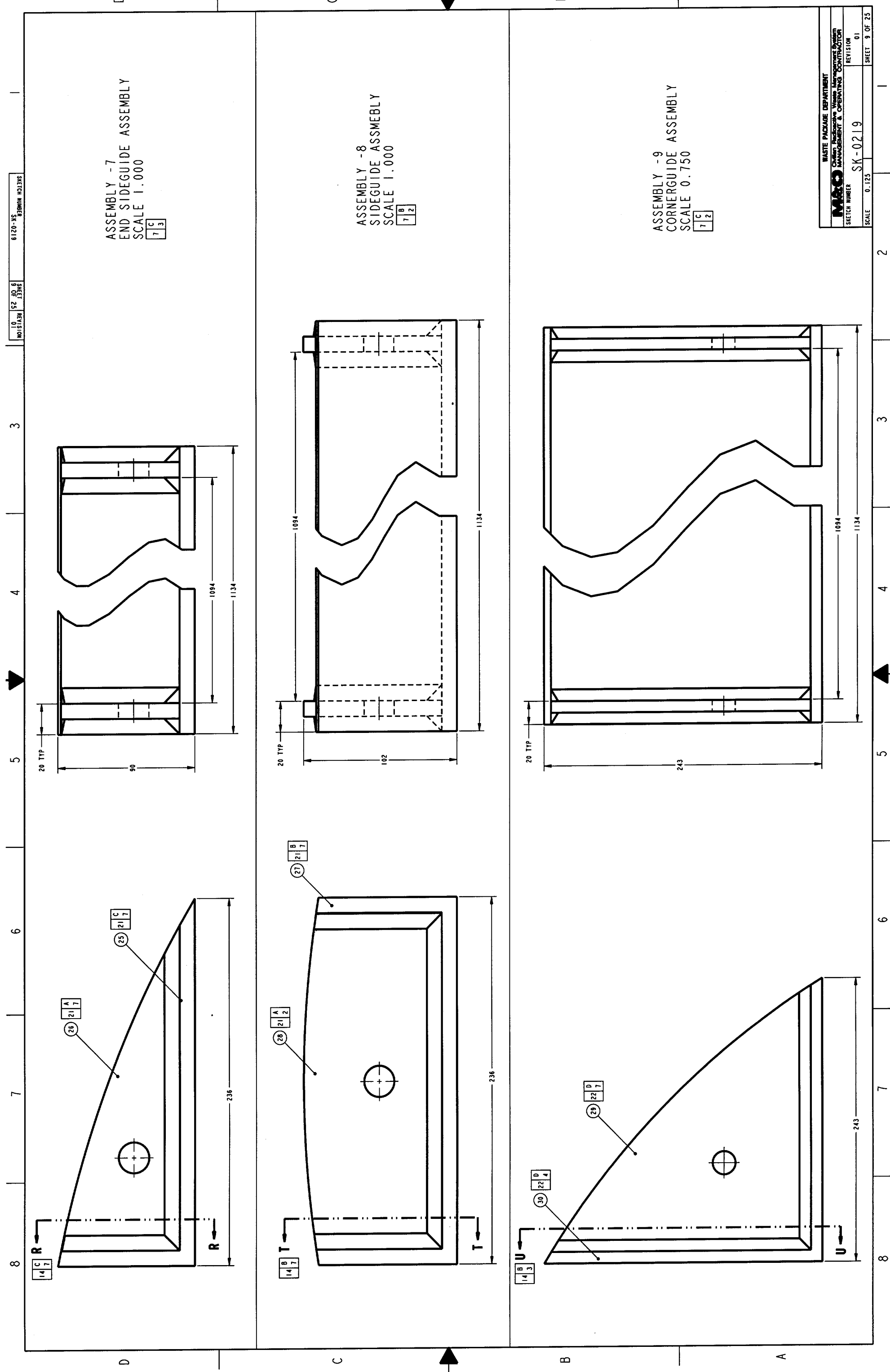


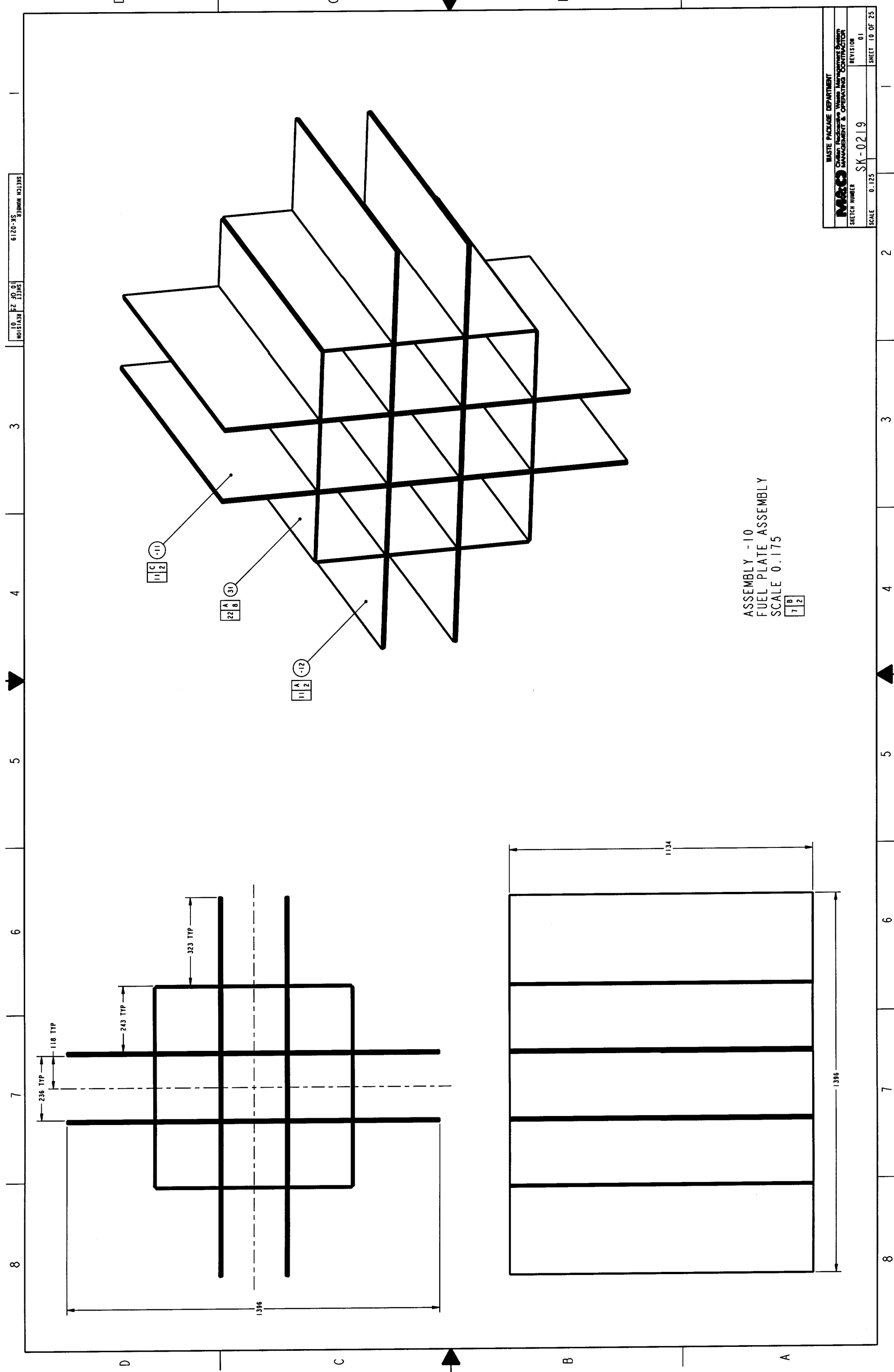


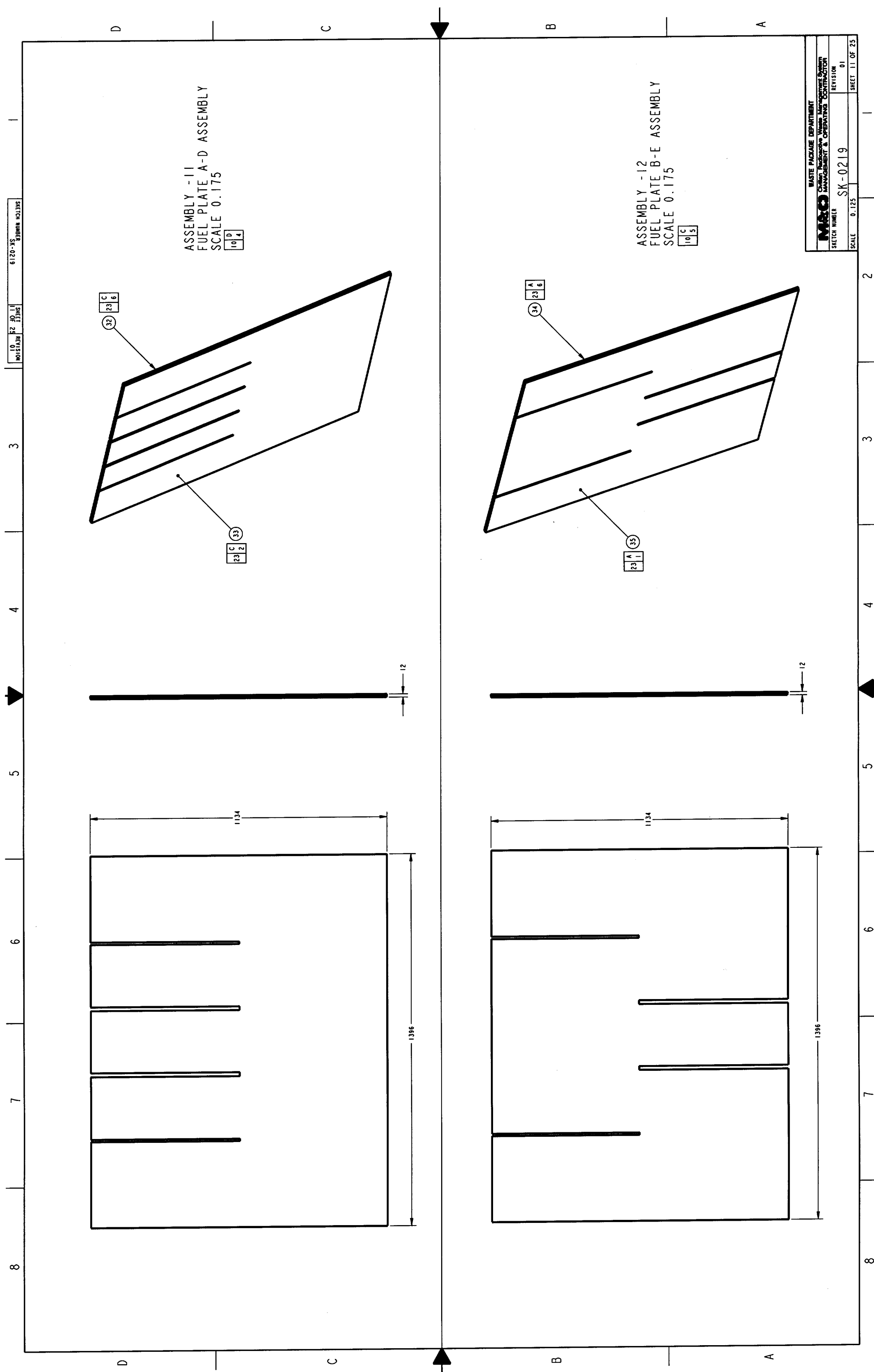


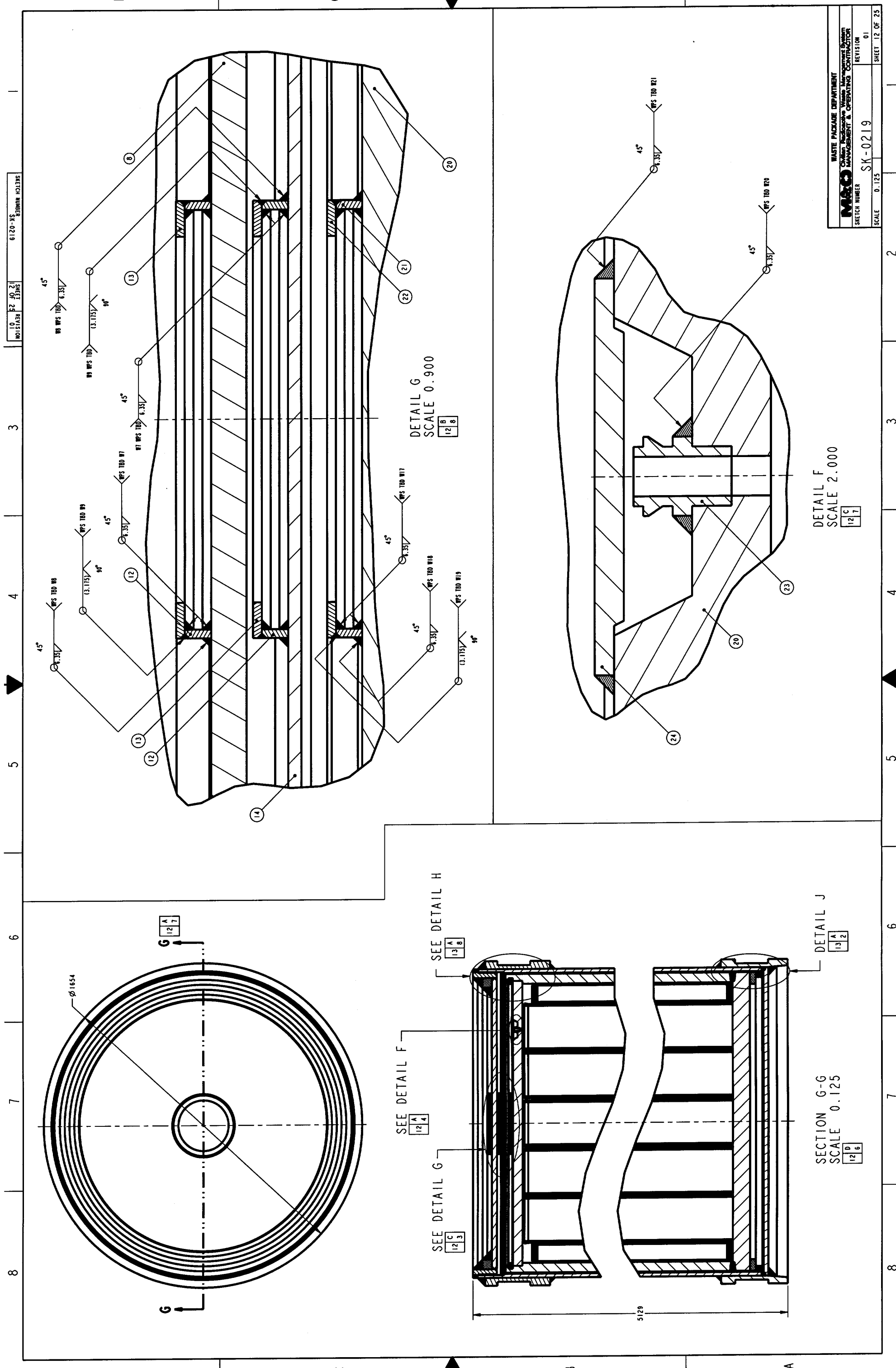


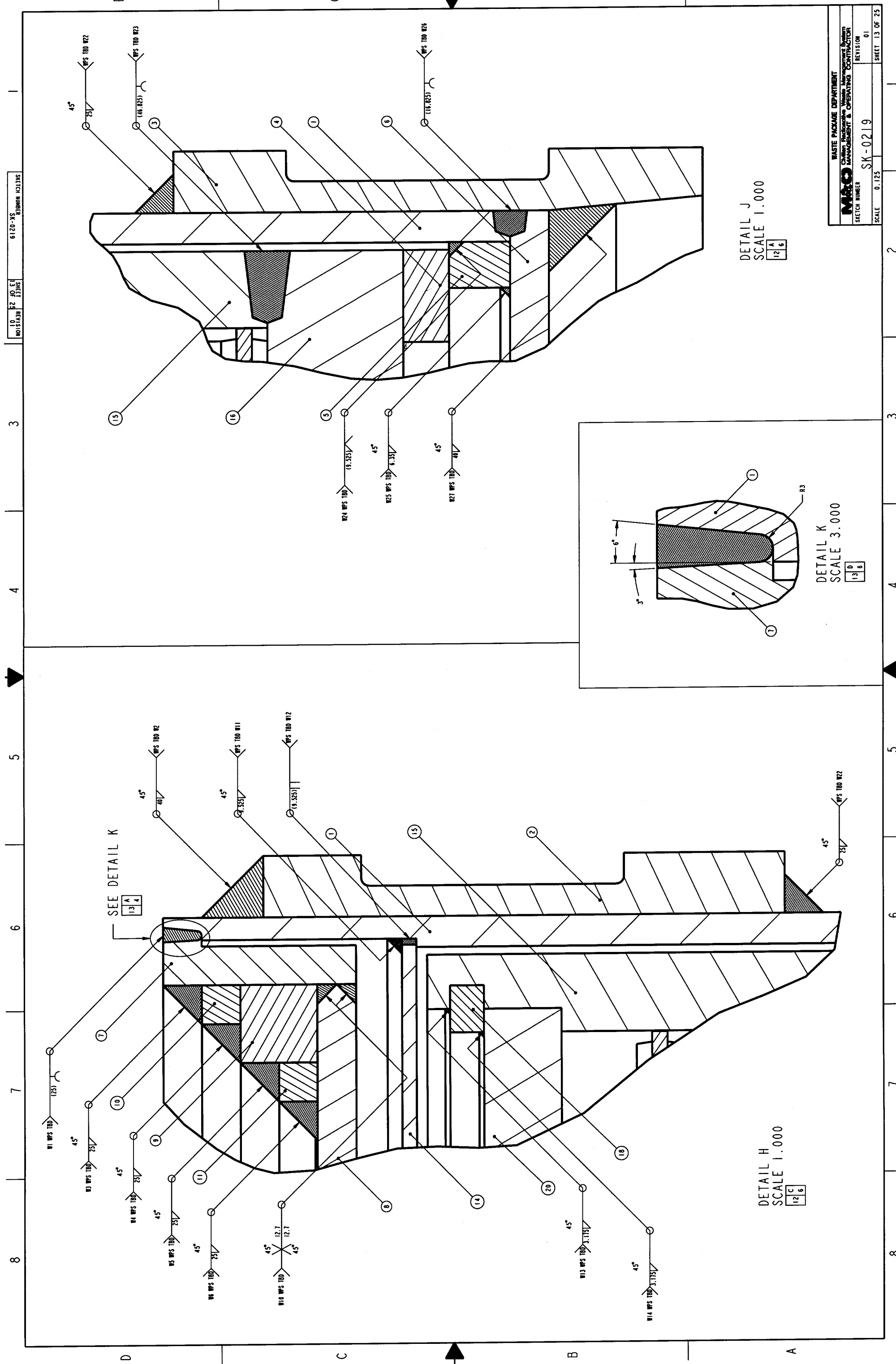


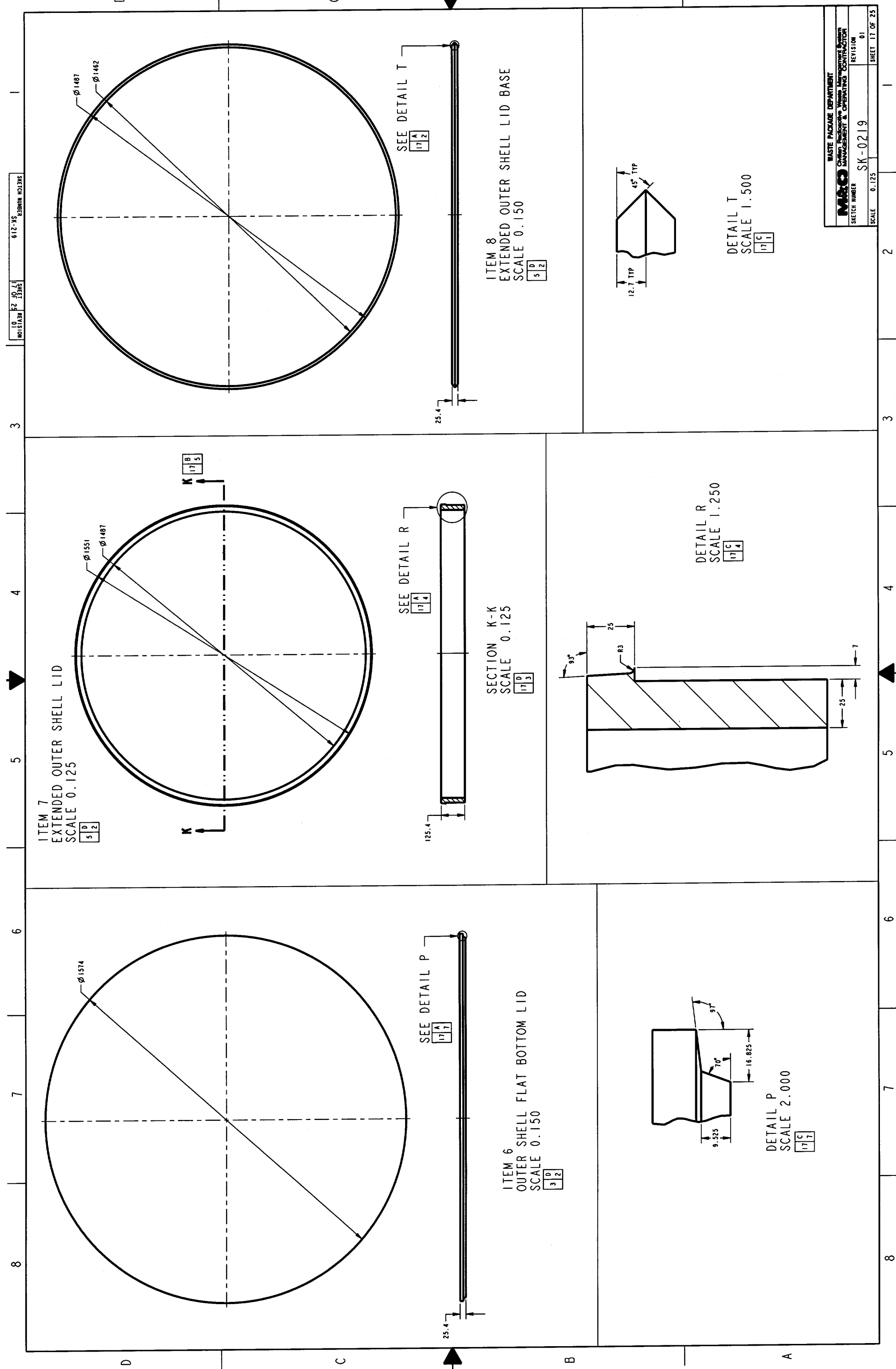


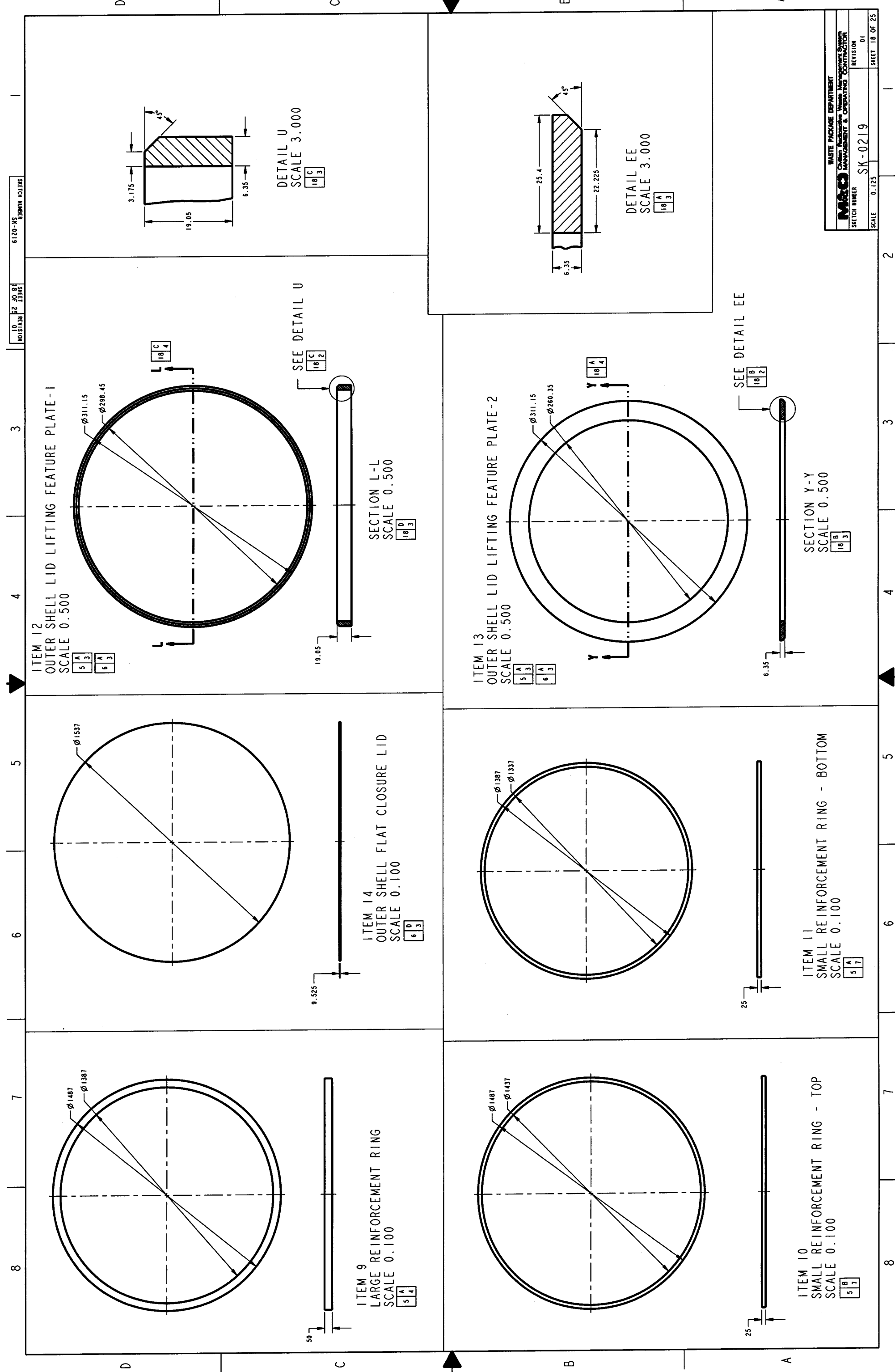


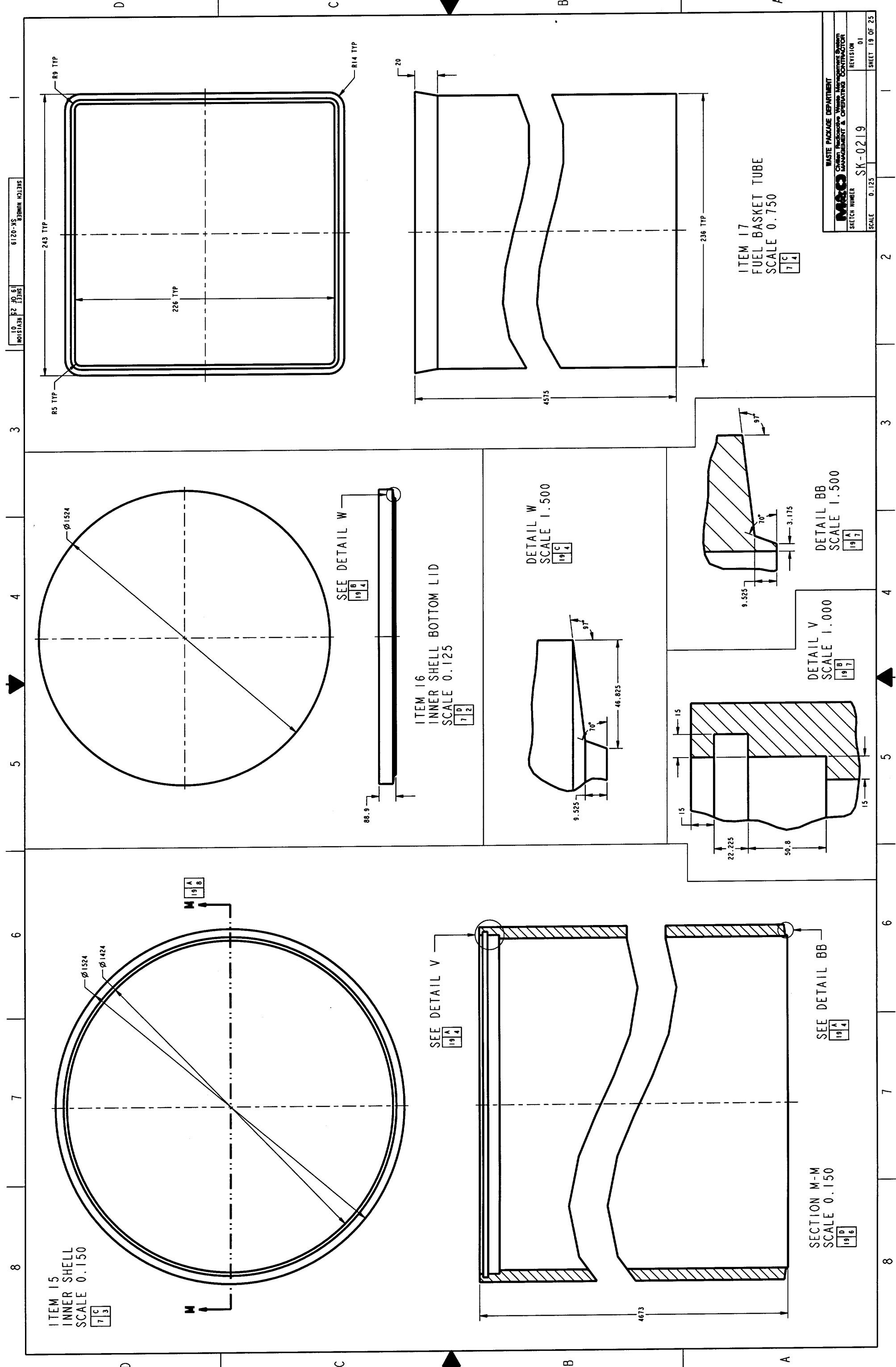


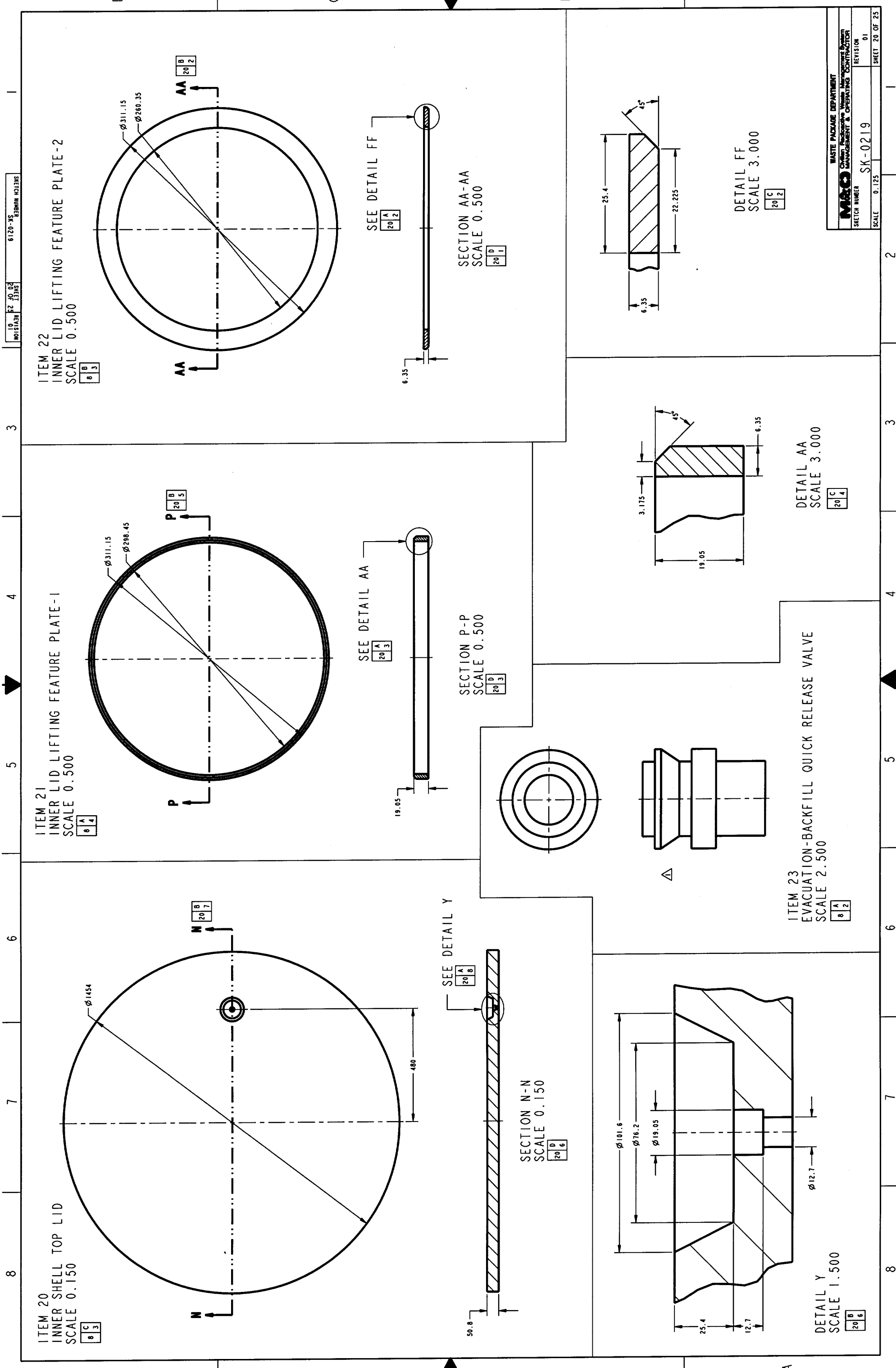


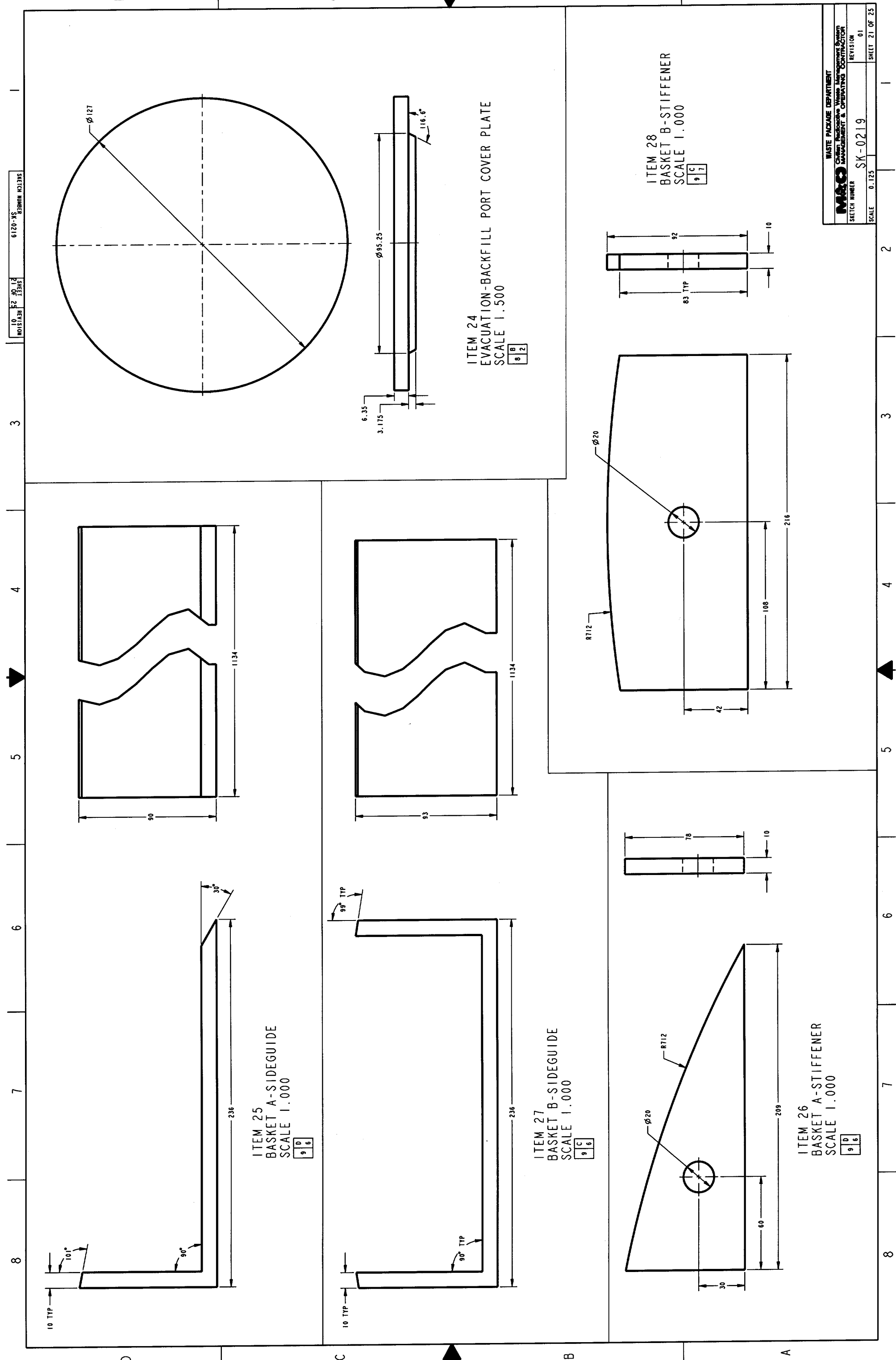


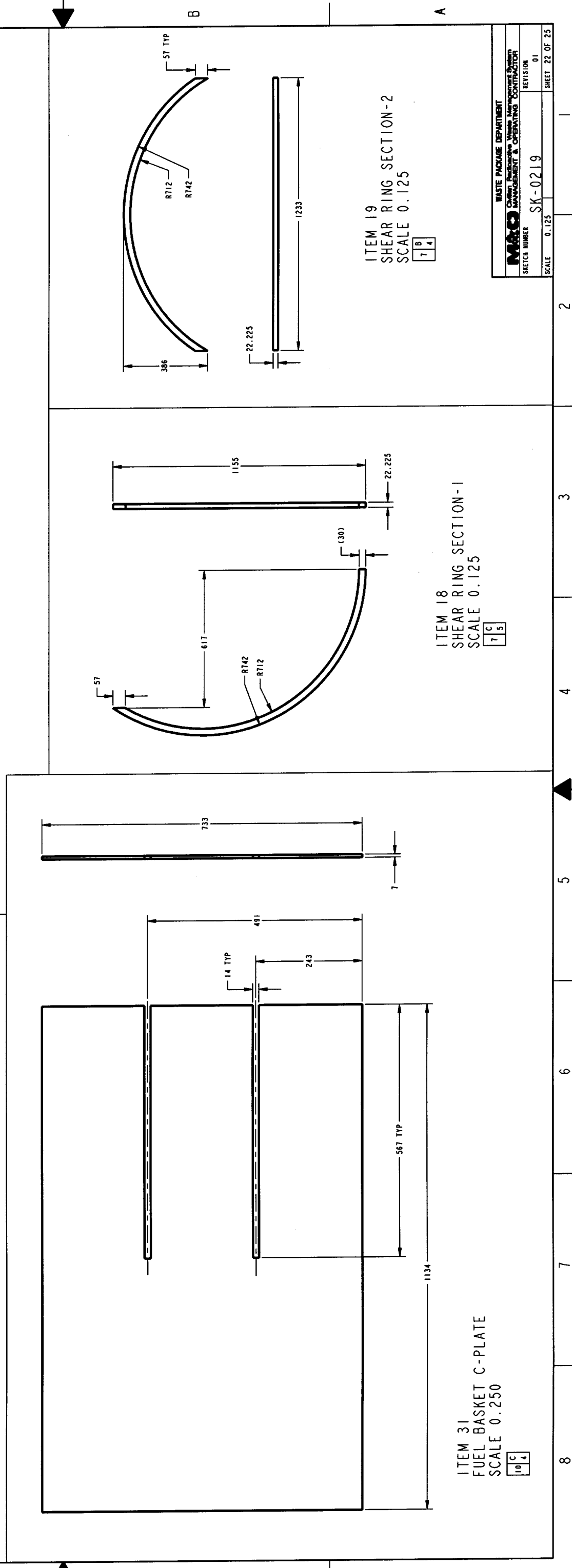
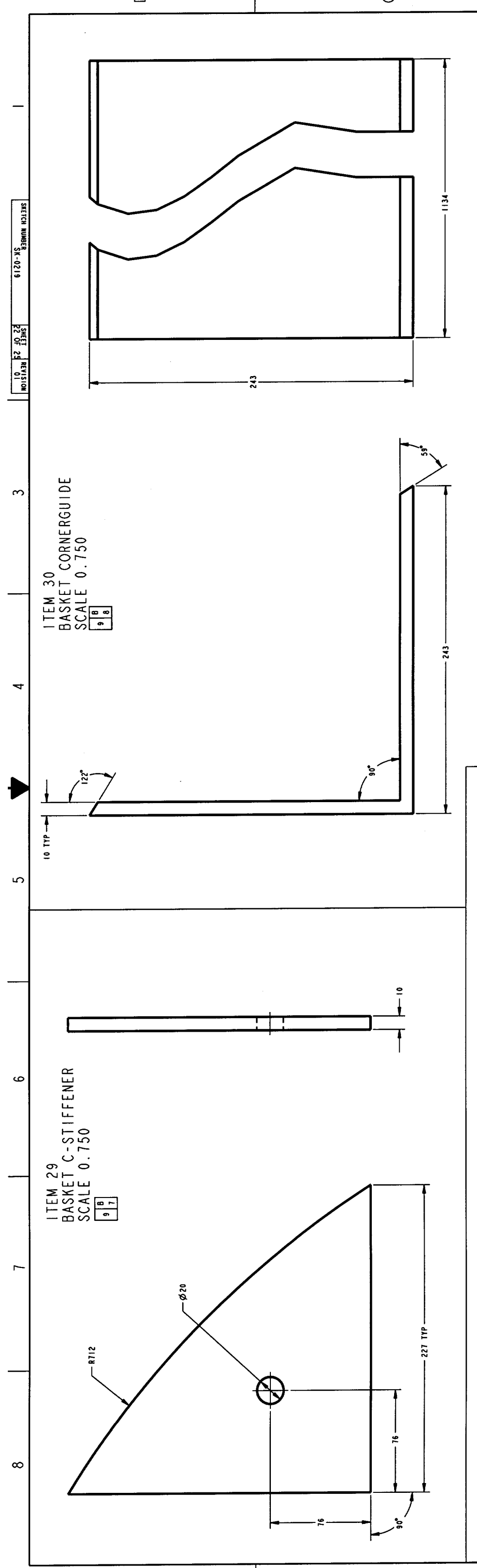


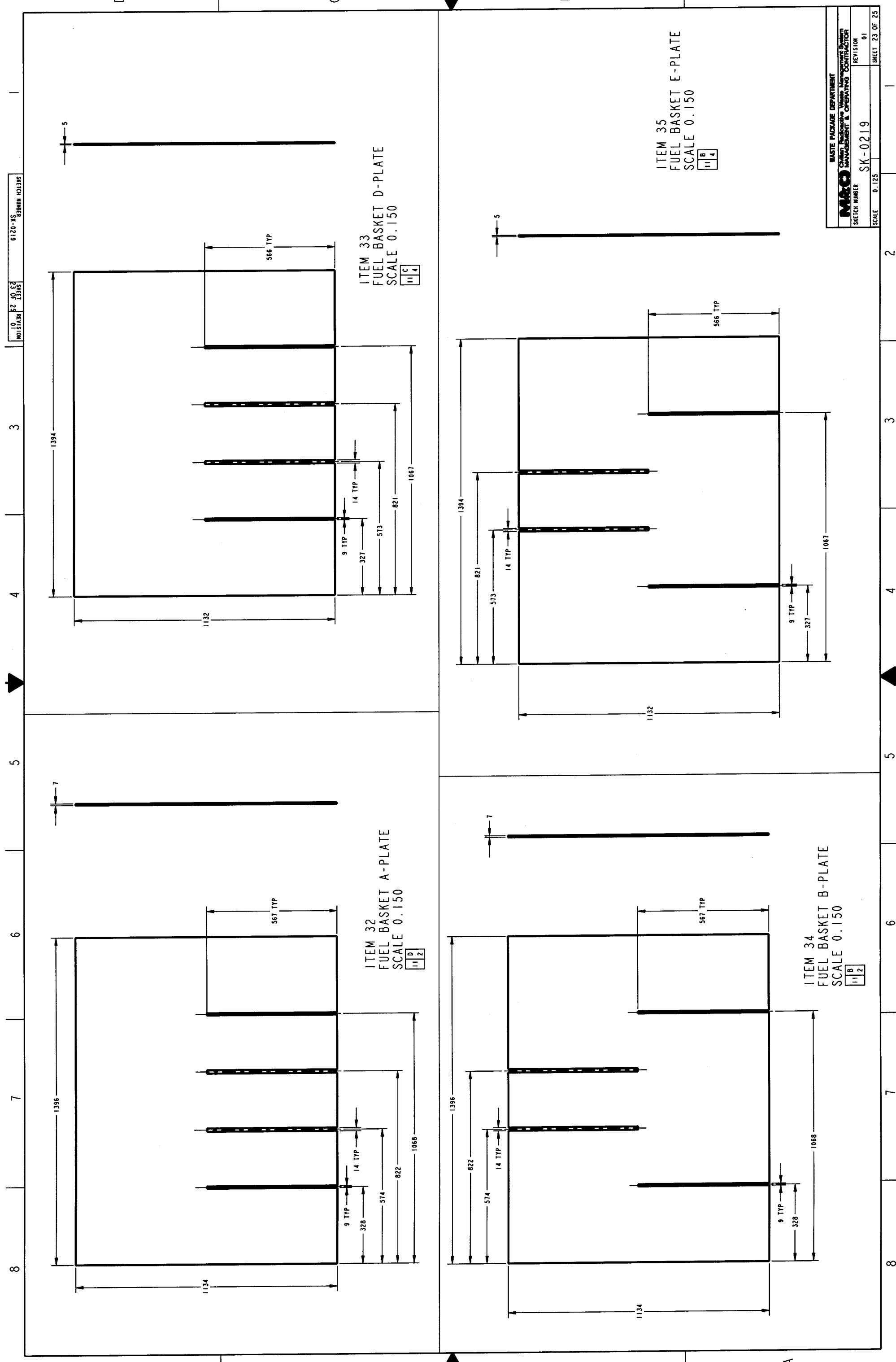












ITEM	REFERENCE	DESCRIPTION		REVISION HISTORY
		ZONE	REV	
-1	21-PWR WASTE PACKAGE ASSEMBLY	D	-	CONTINUED FROM SHEET 1
-2	OUTER SHELL ASSEMBLY		-	01 ADDED SECTION V
1	OUTER SHELL		-	01 ADDED ITEM 18 IN ZONES C5-7, B1-13, C8-24, AND A4-22
2	UPPER TRUNNION COLLAR SLEEVE		-	01 ADDED ITEM 19 IN ZONES B4-7, C8-24, AND A2-22
3	LOWER TRUNNION COLLAR SLEEVE		-	01 ITEM 15 WAS ITEM 14 IN ZONES C2-7, C3-13, C5-19, AND C8-24
4	SHELL INTERFACE RING		-	01 ITEM 16 WAS ITEM 15 IN ZONES D1-7, C1-12, B8-13, A4-12, D8-19, AND C8-24
5	INNER SHELL SUPPORT RING		-	01 ITEM 17 WAS ITEM 16 IN ZONES C4-7, A2-19, AND C8-24
6	OUTER SHELL FLAT BOTTOM LID		-	01 ITEM 17 WAS ITEM 16 IN ZONES C4-7, A2-19, AND C8-24
-3	EXTENDED OUTER SHELL LID ASSEMBLY		-	01 4762 WAS 4712
7	EXTENDED OUTER SHELL LID		-	01 88-9 WAS 50 IN ZONES A8-7, C5-19, AND C4-24
8	EXTENDED OUTER SHELL LID BASE		-	01 ITEM 20 WAS ITEM 17 IN ZONES C3-8, C1-12, B8-13, A4-12, D8-20, AND C8-24
9	LARGE REINFORCEMENT RING		-	01 ADDED DETAIL DD TO SHOW CALLOUTS OF ITEM 21 AND ITEM 22
10	SMALL REINFORCEMENT RING - TOP		-	01 ADDED DETAIL DD CALLOUT
11	SMALL REINFORCEMENT RING - BOTTOM		-	01 ADDED ITEM 20 CALLOUT
12	OUTER SHELL LID LIFTING FEATURE PLATE-1		-	01 ADDED ITEM 22
13	OUTER SHELL LID LIFTING FEATURE PLATE-2		-	01 ITEM 23 WAS ITEM 19 IN ZONES A2-8, A4-12, A6-20, AND B8-24
-4	OUTER SHELL FLAT CLOSURE LID ASSEMBLY		-	01 ITEM 24 WAS ITEM 20 IN ZONES B2-8, B5-12, B2-21, AND B8-24
14	OUTER SHELL FLAT CLOSURE LID		-	01 76-2 WAS 77
15	INNER SHELL LID LIFTING FEATURE PLATE-1		-	01 ADDED 20 TYP IN ZONES B5-9, C5-9, AND D5-9
16	INNER SHELL LID LIFTING FEATURE PLATE-2		-	01 ITEM 25 WAS ITEM 22 IN ZONES D7-9, C7-21, AND B8-24
17	INNER SHELL BOTTOM LID		-	01 ITEM 26 WAS ITEM 22 IN ZONES D7-9, C7-21, AND B8-24
18	FUEL BASKET TUBE		-	01 ITEM 27 WAS ITEM 24 IN ZONES C7-9, B1-21, AND B8-24
19	NEUTRONIT A 978		-	01 ITEM 28 WAS ITEM 24 IN ZONES C7-9, B1-21, AND B8-24
20	NEUTRONIT B 978		-	01 ITEM 29 WAS ITEM 23 IN ZONES B7-21, C6-9, AND B8-24
21	INNER SHELL ASSEMBLY		-	01 ITEM 30 WAS ITEM 26 IN ZONES B8-9, D3-22, AND B8-24
22	INNER SHELL FLAT CLOSURE LID ASSEMBLY		-	01 ITEM 31 WAS ITEM 27 IN ZONES C4-10, A8-22, AND B8-24
23	INNER SHELL FLAT CLOSURE LID		-	01 ITEM 32 WAS ITEM 29 IN ZONES C4-11, C2-23, AND B8-24
24	EVACUATION-BACKFLIP PORT COVER PLATE		-	01 ITEM 33 WAS ITEM 28 IN ZONES D2-11, C6-23, AND B8-24
-6	INNER SHELL TOP LID ASSEMBLY		-	01 ITEM 34 WAS ITEM 31 IN ZONES B4-11, B1-23, AND A8-24
25	INNER SHELL TOP LID		-	01 ITEM 35 WAS ITEM 30 IN ZONES B2-11, A6-23, AND A8-24
26	INNER LID LIFTING FEATURE PLATE-1		-	01 6-35 WAS 12-7 IN ZONES D4-12 AND D2-12
27	INNER LID LIFTING FEATURE PLATE-2		-	01 03-12 01 ADDED W9 IN 2 PLACES
28	EVACUATION-BACKFLIP PORT COVER PLATE		-	01 D8-25 01 ADDED WELD 9
-9	EVACUATION-BACKFLIP PORT COVER PLATE		-	01 03-12 01 ADDED W7 IN 2 PLACES
29	BASKET A-STIFFENER		-	01 B4-12 01 ADDED W19
30	BASKET B-STIFFENER		-	01 C0-12 01 ADDED ITEM 13 CALLOUT IN ZONES D2-12 AND D5-12
-8	BASKET CORNERGUIDE		-	01 C2-12 01 ITEM 21 WAS ITEM 18
31	SIDEGUIDE ASSEMBLY		-	01 C8-25 01 ADDED WELD 19
32	SIDEGUIDE ASSEMBLY		-	01 C4-12 01 W18 WAS W14
33	CORNERGUIDE ASSEMBLY		-	01 C8-25 01 WELD 18 WAS WELD 14
-10	CORNERGUIDE ASSEMBLY		-	01 C4-12 01 6-35 WAS 12-7
34	FUEL PLATE ASSEMBLY		-	01 C4-12 01 W17 WAS W13
35	FUEL PLATE ASSEMBLY		-	01 C8-25 01 WELD 17 WAS WELD 13
-12	FUEL PLATE ASSEMBLY		-	01 C4-12 01 W18 WAS W14
36	FUEL PLATE ASSEMBLY		-	01 C8-25 01 WELD 18 WAS WELD 14
37	FUEL PLATE ASSEMBLY		-	01 C4-12 01 W17 WAS W13
38	FUEL PLATE ASSEMBLY		-	01 C8-25 01 WELD 17 WAS WELD 13
39	FUEL PLATE ASSEMBLY		-	01 C4-12 01 W18 WAS W14
40	FUEL PLATE ASSEMBLY		-	01 C8-25 01 WELD 18 WAS WELD 14
41	FUEL PLATE ASSEMBLY		-	01 C4-12 01 W17 WAS W13
42	FUEL PLATE ASSEMBLY		-	01 C8-25 01 WELD 17 WAS WELD 13
43	FUEL PLATE ASSEMBLY		-	01 C4-12 01 W18 WAS W14
44	FUEL PLATE ASSEMBLY		-	01 C8-25 01 WELD 18 WAS WELD 14
45	FUEL PLATE ASSEMBLY		-	01 C4-12 01 W17 WAS W13
46	FUEL PLATE ASSEMBLY		-	01 C8-25 01 WELD 17 WAS WELD 13
47	FUEL PLATE ASSEMBLY		-	01 C4-12 01 W18 WAS W14
48	FUEL PLATE ASSEMBLY		-	01 C8-25 01 WELD 18 WAS WELD 14
49	FUEL PLATE ASSEMBLY		-	01 C4-12 01 W17 WAS W13
50	FUEL PLATE ASSEMBLY		-	01 C8-25 01 WELD 17 WAS WELD 13
51	FUEL PLATE ASSEMBLY		-	01 C4-12 01 W18 WAS W14
52	FUEL PLATE ASSEMBLY		-	01 C8-25 01 WELD 18 WAS WELD 14
53	FUEL PLATE ASSEMBLY		-	01 C4-12 01 W17 WAS W13
54	FUEL PLATE ASSEMBLY		-	01 C8-25 01 WELD 17 WAS WELD 13
55	FUEL PLATE ASSEMBLY		-	01 C4-12 01 W18 WAS W14
56	FUEL PLATE ASSEMBLY		-	01 C8-25 01 WELD 18 WAS WELD 14
57	FUEL PLATE ASSEMBLY		-	01 C4-12 01 W17 WAS W13
58	FUEL PLATE ASSEMBLY		-	01 C8-25 01 WELD 17 WAS WELD 13
59	FUEL PLATE ASSEMBLY		-	01 C4-12 01 W18 WAS W14
60	FUEL PLATE ASSEMBLY		-	01 C8-25 01 WELD 18 WAS WELD 14
61	FUEL PLATE ASSEMBLY		-	01 C4-12 01 W17 WAS W13
62	FUEL PLATE ASSEMBLY		-	01 C8-25 01 WELD 17 WAS WELD 13
63	FUEL PLATE ASSEMBLY		-	01 C4-12 01 W18 WAS W14
64	FUEL PLATE ASSEMBLY		-	01 C8-25 01 WELD 18 WAS WELD 14
65	FUEL PLATE ASSEMBLY		-	01 C4-12 01 W17 WAS W13
66	FUEL PLATE ASSEMBLY		-	01 C8-25 01 WELD 17 WAS WELD 13
67	FUEL PLATE ASSEMBLY		-	01 C4-12 01 W18 WAS W14
68	FUEL PLATE ASSEMBLY		-	01 C8-25 01 WELD 18 WAS WELD 14
69	FUEL PLATE ASSEMBLY		-	01 C4-12 01 W17 WAS W13
70	FUEL PLATE ASSEMBLY		-	01 C8-25 01 WELD 17 WAS WELD 13
71	FUEL PLATE ASSEMBLY		-	01 C4-12 01 W18 WAS W14
72	FUEL PLATE ASSEMBLY		-	01 C8-25 01 WELD 18 WAS WELD 14
73	FUEL PLATE ASSEMBLY		-	01 C4-12 01 W17 WAS W13
74	FUEL PLATE ASSEMBLY		-	01 C8-25 01 WELD 17 WAS WELD 13
75	FUEL PLATE ASSEMBLY		-	01 C4-12 01 W18 WAS W14
76	FUEL PLATE ASSEMBLY		-	01 C8-25 01 WELD 18 WAS WELD 14
77	FUEL PLATE ASSEMBLY		-	01 C4-12 01 W17 WAS W13
78	FUEL PLATE ASSEMBLY		-	01 C8-25 01 WELD 17 WAS WELD 13
79	FUEL PLATE ASSEMBLY		-	01 C4-12 01 W18 WAS W14
80	FUEL PLATE ASSEMBLY		-	01 C8-25 01 WELD 18 WAS WELD 14
81	FUEL PLATE ASSEMBLY		-	01 C4-12 01 W17 WAS W13
82	FUEL PLATE ASSEMBLY		-	01 C8-25 01 WELD 17 WAS WELD 13
83	FUEL PLATE ASSEMBLY		-	01 C4-12 01 W18 WAS W14
84	FUEL PLATE ASSEMBLY		-	01 C8-25 01 WELD 18 WAS WELD 14
85	FUEL PLATE ASSEMBLY		-	01 C4-12 01 W17 WAS W13
86	FUEL PLATE ASSEMBLY		-	01 C8-25 01 WELD 17 WAS WELD 13
87	FUEL PLATE ASSEMBLY		-	01 C4-12 01 W18 WAS W14
88	FUEL PLATE ASSEMBLY		-	01 C8-25 01 WELD 18 WAS WELD 14
89	FUEL PLATE ASSEMBLY		-	01 C4-12 01 W17 WAS W13
90	FUEL PLATE ASSEMBLY		-	01 C8-25 01 WELD 17 WAS WELD 13
91	FUEL PLATE ASSEMBLY		-	01 C4-12 01 W18 WAS W14
92	FUEL PLATE ASSEMBLY		-	01 C8-25 01 WELD 18 WAS WELD 14
93	FUEL PLATE ASSEMBLY		-	01 C4-12 01 W17 WAS W13
94	FUEL PLATE ASSEMBLY		-	01 C8-25 01 WELD 17 WAS WELD 13
95	FUEL PLATE ASSEMBLY		-	01 C4-12 01 W18 WAS W14
96	FUEL PLATE ASSEMBLY		-	01 C8-25 01 WELD 18 WAS WELD 14
97	FUEL PLATE ASSEMBLY		-	01 C4-12 01 W17 WAS W13
98	FUEL PLATE ASSEMBLY		-	01 C8-25 01 WELD 17 WAS WELD 13
99	FUEL PLATE ASSEMBLY		-	01 C4-12 01 W18 WAS W14
100	FUEL PLATE ASSEMBLY		-	01 C8-25 01 WELD 18 WAS WELD 14
101	FUEL PLATE ASSEMBLY		-	01 C4-12 01 W17 WAS W13
102	FUEL PLATE ASSEMBLY		-	01 C8-25 01 WELD 17 WAS WELD 13
103	FUEL PLATE ASSEMBLY		-	01 C4-12 01 W18 WAS W14
104	FUEL PLATE ASSEMBLY		-	01 C8-25 01 WELD 18 WAS WELD 14
105	FUEL PLATE ASSEMBLY		-	01 C4-12 01 W17 WAS W13
106	FUEL PLATE ASSEMBLY		-	01 C8-25 01 WELD 17 WAS WELD 13
107	FUEL PLATE ASSEMBLY		-	01 C4-12 01 W18 WAS W14
108	FUEL PLATE ASSEMBLY		-	01 C8-25 01 WELD 18 WAS WELD 14
109	FUEL PLATE ASSEMBLY		-	01 C4-12 01 W17 WAS W13
110	FUEL PLATE ASSEMBLY		-	01 C8-25 01 WELD 17 WAS WELD 13
111	FUEL PLATE ASSEMBLY		-	01 C4-12 01 W18 WAS W14
112	FUEL PLATE ASSEMBLY		-	01 C8-25 01 WELD 18 WAS WELD 14
113	FUEL PLATE ASSEMBLY		-	01 C4-12 01 W17 WAS W13
114	FUEL PLATE ASSEMBLY		-	01 C8-25 01 WELD 17 WAS WELD 13
115	FUEL PLATE ASSEMBLY</			

3

4

5

6

7

8

WELD LIST			
WELD NUMBER	WELD TYPE	MATERIAL	WELD SIZE
1	GROOVE	SFA-5.14 NO6022	7.8
2	FILLET	SFA-5.14 NO6022	35
3	FILLET	SFA-5.14 NO6022	13
4	FILLET	SFA-5.14 NO6022	12
5	FILLET	SFA-5.14 NO6022	0.09
10	GROOVE	SFA-5.14 NO6022	3.3
6	FILLET	SFA-5.14 NO6022	11
7	FILLET	SFA-5.14 NO6022	0.16
8	FILLET	SFA-5.14 NO6022	0.17
9	GROOVE	SFA-5.14 NO6022	2
10	GROOVE	SFA-5.14 NO6022	12
11	FILLET	SFA-5.14 NO6022	1.9
12	SQUARE	SFA-5.14 NO6022	1.6
13	FILLET	SFA-5.9 S31680	0.18
14	FILLET	SFA-5.9 S31680	0.18
15	SQUARE	SFA-5.9 S31680	0.001
16	SQUARE	SFA-5.9 S31680	0.002
17	FILLET	SFA-5.9 S31680	2
18	FILLET	SFA-5.9 S31680	0.16
19	GROOVE	SFA-5.9 S31680	0.08
20	FILLET	SFA-5.9 S31680	0.01
21	FILLET	SFA-5.9 S31680	0.07
22	FILLET	SFA-5.14 NO6022	14
23	GROOVE	SFA-5.9 S31680	40
24	GROOVE	SFA-5.14 NO6022	1.9
25	FILLET	SFA-5.14 NO6022	0.81
26	GROOVE	SFA-5.14 NO6022	13
27	FILLET	SFA-5.14 NO6022	37
28	FILLET	SFA-5.18 K10126	0.11
29	FILLET	SFA-5.18 K10126	64
30	FILLET	SFA-5.14 NO6022	0.17
TOTAL CARBON STEEL WELDS		SFA-5.18 K10126	34
TOTAL ALLOY 22 WELDS	-	SFA-5.14 NO6022	182
TOTAL 316 WELDS	-	SFA-5.9 S31680	41

NOTES:

△ INFORMATION FOR THE EVACUATION-BACKFILL VALVE IS TBD.

△ THE 21-PWR WASTE PACKAGE CONFIGURATION WITH ABSORBER PLATES IS IDENTICAL TO THE 21-PWR WASTE PACKAGE CONFIGURATION WITH CONTROL RODS, EXCEPT FOR THE MATERIAL COMPOSITION OF THE FUEL BASKET A, B, AND C PLATES. ALL INFORMATION PROVIDED IN THIS TABLE IS FOR THE 21-PWR WASTE PACKAGE CONFIGURATION WITH ABSORBER PLATES, UNLESS OTHERWISE NOTED.

△ GEOMETRY FOR THE 21-PWR WASTE PACKAGE CONFIGURATION WITH CONTROL RODS.

△ THE 21-PWR WASTE CONTAINER CAVITY SIZE DETERMINATION IS FOR THE 21-PWR WASTE PACKAGE. ALL INFORMATION PROVIDED IN THIS TABLE IS FOR THE 21-PWR WASTE PACKAGE CONFIGURATION WITH ABSORBER PLATES, UNLESS OTHERWISE NOTED.

△ WELD 15 SQUARE BUTT WELD IS PLACED ON THE EXPOSED SURFACES ABOVE THE OPEN CAVITY CREATED BETWEEN THE MATING SURFACES OF BOTH SHEAR RING SECTION-1 AND SECTION-2. THIS WELD IS INTENDED TO INSURE ISOLATION OF THE INTERIOR OF THE INNER SHELL ASSEMBLY FROM EXTERNAL ENVIRONMENTS.

△ WELD 16 SQUARE BUTT WELDS ARE PLACED ON THE EXPOSED SURFACES ABOVE THE OPEN CAVITY CREATED BETWEEN THE MATING SURFACES OF THE SHEAR RING SECTION-1 AND THE SHEAR RING SECTION-2 COMPONENTS. THIS WELD IS INTENDED TO INSURE ISOLATION OF THE INTERIOR OF THE INNER SHELL ASSEMBLY FROM EXTERNAL ENVIRONMENTS.

△ WELD 15 WELD 22 WAS WELD 17

△ WELD 22 WAS WELD 11

△ WELD 12 WAS WELD 11

△ WELD 10 IN 2 PLACES

△ WELD 11 WAS WELD 10

△ WELD 12 WAS WELD 19

△ WELD 13 WAS WELD 19

△ WELD 14 WAS WELD 20

△ WELD 15 WAS WELD 21

△ WELD 16 WAS WELD 19

△ WELD 17 WAS WELD 19

△ WELD 18 WAS WELD 20

△ WELD 19 WAS WELD 21

△ WELD 20 WAS WELD 19

△ WELD 21 WAS WELD 19

△ WELD 22 WAS WELD 19

△ WELD 23 WAS WELD 18

△ WELD 24 WAS WELD 22

△ WELD 25 WAS WELD 20

△ WELD 26 WAS WELD 21

△ WELD 27 WAS WELD 22

△ WELD 28 WAS WELD 21

△ WELD 29 WAS WELD 23

△ WELD 30 WAS WELD 16

△ WELD 31 WAS 371

△ WELD 32 WAS 27 IN 3 PLACES

△ WELD 33 WAS 13 IN 2 PLACES

△ WELD 34 WAS 161

△ WELD 35 WAS 6.4

△ WELD 36 WAS W22

△ WELD 37 WAS W23

△ WELD 38 WAS W24

△ WELD 39 WAS W25

△ WELD 40 WAS W26

△ WELD 41 WAS W27

△ WELD 42 WAS W28

△ WELD 43 WAS W29

△ WELD 44 WAS W30

△ WELD 45 WAS W31

△ WELD 46 WAS W32

△ WELD 47 WAS W33

△ WELD 48 WAS W34

△ WELD 49 WAS W35

△ WELD 50 WAS W36

△ WELD 51 WAS W37

△ WELD 52 WAS W38

△ WELD 53 WAS W39

△ WELD 54 WAS W40

△ WELD 55 WAS W41

△ WELD 56 WAS W42

△ WELD 57 WAS W43

△ WELD 58 WAS W44

△ WELD 59 WAS W45

△ WELD 60 WAS W46

△ WELD 61 WAS W47

△ WELD 62 WAS W48

△ WELD 63 WAS W49

△ WELD 64 WAS W50

△ WELD 65 WAS W51

△ WELD 66 WAS W52

△ WELD 67 WAS W53

△ WELD 68 WAS W54

△ WELD 69 WAS W55

△ WELD 70 WAS W56

△ WELD 71 WAS W57

△ WELD 72 WAS W58

△ WELD 73 WAS W59

△ WELD 74 WAS W60

△ WELD 75 WAS W61

△ WELD 76 WAS W62

△ WELD 77 WAS W63

△ WELD 78 WAS W64

△ WELD 79 WAS W65

△ WELD 80 WAS W66

△ WELD 81 WAS W67

△ WELD 82 WAS W68

△ WELD 83 WAS W69

△ WELD 84 WAS W70

△ WELD 85 WAS W71

△ WELD 86 WAS W72

△ WELD 87 WAS W73

△ WELD 88 WAS W74

△ WELD 89 WAS W75

△ WELD 90 WAS W76

△ WELD 91 WAS W77

△ WELD 92 WAS W78

△ WELD 93 WAS W79

△ WELD 94 WAS W80

△ WELD 95 WAS W81

△ WELD 96 WAS W82

△ WELD 97 WAS W83

△ WELD 98 WAS W84

△ WELD 99 WAS W85

△ WELD 100 WAS W86

△ WELD 101 WAS W87

△ WELD 102 WAS W88

△ WELD 103 WAS W89

△ WELD 104 WAS W90

△ WELD 105 WAS W91

△ WELD 106 WAS W92

△ WELD 107 WAS W93

△ WELD 108 WAS W94

△ WELD 109 WAS W95

△ WELD 110 WAS W96

△ WELD 111 WAS W97

△ WELD 112 WAS W98

△ WELD 113 WAS W99

△ WELD 114 WAS W100

△ WELD 115 WAS W101

△ WELD 116 WAS W102

△ WELD 117 WAS W103

△ WELD 118 WAS W104

△ WELD 119 WAS W105

△ WELD 120 WAS W106

△ WELD 121 WAS W107

△ WELD 122 WAS W108

△ WELD 123 WAS W109

△ WELD 124 WAS W110

△ WELD 125 WAS W111

△ WELD 126 WAS W112

△ WELD 127 WAS W113

△ WELD 128 WAS W114

△ WELD 129 WAS W115

△ WELD 130 WAS W116

△ WELD 131 WAS W117

△ WELD 132 WAS W118

△ WELD 133 WAS W119

△ WELD 134 WAS W120

△ WELD 135 WAS W121

△ WELD 136 WAS W122

△ WELD 137 WAS W123

△ WELD 138 WAS W124

△ WELD 139 WAS W125

△ WELD 140 WAS W126

△ WELD 141 WAS W127

△ WELD 142 WAS W128

△ WELD 143 WAS W129

△ WELD 144 WAS W130

△ WELD 145 WAS W131

△ WELD 146 WAS W132

△ WELD 147 WAS W133

△ WELD 148 WAS W134

△ WELD 149 WAS W135

△ WELD 150 WAS W136

△ WELD 151 WAS W137

△ WELD 152 WAS W138

△ WELD 153 WAS W139

△ WELD 154 WAS W140

△ WELD 155 WAS W141

△ WELD 156 WAS W142

△ WELD 157 WAS W143

△ WELD 158 WAS W144

△ WELD 159 WAS W145

△ WELD 160 WAS W146

△ WELD 161 WAS W147

△ WELD 162 WAS W148

△ WELD 163 WAS W149

△ WELD 164 WAS W150

△ WELD 165 WAS W151

△ WELD 166 WAS W152

△ WELD 167 WAS W153

△ WELD 168 WAS W154

△ WELD 169 WAS W155

△ WELD 170 WAS W156

△ WELD 171 WAS W157

△ WELD 172 WAS W158

△ WELD 173 WAS W159

△ WELD 174 WAS W160

△ WELD 175 WAS W161

△ WELD 176 WAS W162

△ WELD 177 WAS W163

△ WELD 178 WAS W164

△ WELD 179 WAS W165

△ WELD 180 WAS W166

△ WELD 181 WAS W167

△ WELD 182 WAS W168

△ WELD 183 WAS W169

△ WELD 184 WAS W170

△ WELD 185 WAS W171

△ WELD 186 WAS W172

△ WELD 187 WAS W173

△ WELD 188 WAS W174

△ WELD 189 WAS W175

△ WELD 190 WAS W176

△ WELD 191 WAS W177

△ WELD 192 WAS W178

△ WELD 193 WAS W179

△ WELD 194 WAS W180

△ WELD 195 WAS W181

△ WELD 196 WAS W182

△ WELD 197 WAS W183

△ WELD 198 WAS W184

△ WELD 199 WAS W185

△ WELD 200 WAS W186

△ WELD 201 WAS W187

△ WELD 202 WAS W188

△ WELD 203 WAS W189

△ WELD 204 WAS W190

△ WELD 205 WAS W191

△ WELD 206 WAS W192

△ WELD 207 WAS W193

△ WELD 208 WAS W194

△ WELD 209 WAS W195

△ WELD 210 WAS W196

△ WELD 211 WAS W197

△ WELD 212 WAS W198

△ WELD 213 WAS W199

△ WELD 214 WAS W200

△ WELD 215 WAS W201

△ WELD 216 WAS W202

△ WELD 217 WAS W203

△ WELD 218 WAS W204

△ WELD 219 WAS W205

△ WELD 220 WAS W206

△ WELD 221 WAS W207

△ WELD 222 WAS W208

△ WELD 223 WAS W209

△ WELD 224 WAS W210

△ WELD 225 WAS W211

△ WELD 226 WAS W212

△ WELD 227 WAS W213

△ WELD 228 WAS W214

△ WELD 229 WAS W215

△ WELD 230 WAS W216

△ WELD 231 WAS W217

△ WELD 232 WAS W218

△ WELD 233 WAS W219

△ WELD 234 WAS W220

△ WELD 235 WAS W221

△ WELD 236 WAS W222

△ WELD 237 WAS W223

△ WELD 238 WAS W224

△ WELD 239 WAS W225

△ WELD 240 WAS W226

△ WELD 241 WAS W227

△ WELD 242 WAS W228

△ WELD 243 WAS W229

△ WELD 244 WAS W230

△ WELD 245 WAS W231

△ WELD 246 WAS W232

△ WELD 247 WAS W233

△ WELD 248 WAS W234

△ WELD 249 WAS W235

△ WELD 250 WAS W236

△ WELD 251 WAS W237

△ WELD 252 WAS W238

△ WELD 253 WAS W239

△ WELD 254 WAS W240

△ WELD 255 WAS W241

△ WELD 256 WAS W242

△ WELD 257 WAS W243

△ WELD 258 WAS W244

△ WELD 259 WAS W245

△ WELD 260 WAS W246

△ WELD 261 WAS W247

△ WELD 262 WAS W248

△ WELD 263 WAS W249

△ WELD 264 WAS W250

△ WELD 265 WAS W251

△ WELD 266 WAS W252

△ WELD 267 WAS W253

△ WELD 268 WAS W254

△ WELD 269 WAS W255

△ WELD 270 WAS W256

△ WELD 271 WAS W257

△ WELD 272 WAS W258

△ WELD 273 WAS W259

△ WELD 274 WAS W260

△ WELD 275 WAS W261

△ WELD 276 WAS W262

△ WELD 277 WAS W263

△ WELD 278 WAS W264

△ WELD 279 WAS W265

△ WELD 280 WAS W266

△ WELD 281 WAS W267

△ WELD 282 WAS W268

△ WELD 283 WAS W269

△ WELD 284 WAS W270

△ WELD 285 WAS W271

△ WELD 286 WAS W272

△ WELD 287 WAS W273

△ WELD 288 WAS W274

△ WELD 289 WAS W275

△ WELD 290 WAS W276

△ WELD 291 WAS W277

△ WELD 292 WAS W278

△ WELD 293 WAS W279

△ WELD 294 WAS W280

△ WELD 295 WAS W281

△ WELD 296 WAS W282

△ WELD 297 WAS W283

△ WELD 298 WAS W284

△ WELD 299 WAS W285

△ WELD 300 WAS W286

△ WELD 301